

NEUR2BILO: Neural Bilevel Optimization

Justin Dumouchelle^{*1,2}, Esther Julien³, Jannis Kurtz⁴ and
Elias B. Khalil^{1,2}

¹University of Toronto, Canada

²SCALE AI Research Chair in Data-Driven Algorithms for Modern Supply Chains, Canada

³TU Delft, The Netherlands

⁴University of Amsterdam, The Netherlands

February 6, 2024

Abstract

Bilevel optimization deals with nested problems in which a *leader* takes the first decision to minimize their objective function while accounting for a *follower's* best-response reaction. Constrained bilevel problems with integer variables are particularly notorious for their hardness. While exact solvers have been proposed for mixed-integer *linear* bilevel optimization, they tend to scale poorly with problem size and are hard to generalize to the non-linear case. On the other hand, problem-specific algorithms (exact and heuristic) are limited in scope. Under a data-driven setting in which similar instances of a bilevel problem are solved routinely, our proposed framework, NEUR2BILO, embeds a neural network approximation of the leader's or follower's value function, trained via supervised regression, into an easy-to-solve mixed-integer program. NEUR2BILO serves as a heuristic that produces high-quality solutions extremely fast for the bilevel knapsack interdiction problem, the “critical node problem” from network security, a donor-recipient healthcare problem, and discrete network design from transportation planning. These problems are diverse in that they have linear or non-linear objectives/constraints and integer or mixed-integer variables, making NEUR2BILO unique in its versatility.

1 Introduction

A motivating application. Consider the following *discrete network design problem* (DNDP) [50, 51]. A transportation planning authority seeks to minimize the average travel time on a road network represented by a directed graph of nodes N and links A_1 by investing in constructing a set of roads (i.e., links) from a set of options A_2 , subject to a budget B . The planner knows the number of vehicles that travel between

*Corresponding author: justin.dumouchelle@mail.utoronto.ca

any origin-destination (O-D) pair of nodes. A good selection of links should take into account the drivers' reactions to this decision as it is not possible to centrally plan driver routes. One common assumption is that drivers will optimize their O-D paths such that a *user equilibrium* is reached. This is known as *Wardrop's second principle* in the traffic assignment literature, an equilibrium in which "no driver can unilaterally reduce their travel costs by shifting to another route" [44]. This is in contrast to the *system optimum*, an equilibrium in which a central planner dictates each driver's route, an unrealistic assumption which would not require bilevel modelling. A link cost function is used to model the travel time on an edge as a function of traffic. Let $c_{ij} \in \mathbb{R}_+$ be the capacity (vehicles per hour (vph)) of a link and $T_{ij} \in \mathbb{R}_+$ the free-flow travel time (i.e., travel time on the link without congestion). The US Bureau of Public Roads uses the following widely accepted formula to model the travel time $t(y_{ij})$ on a link used by y_{ij} vehicles per hour: $t(y_{ij}) = T_{ij}(1 + 0.15(y_{ij}/c_{ij})^4)$. As the traffic y_{ij} grows to exceed the capacity c_{ij} , a large quartic increase in travel time is incurred [44].

Bilevel optimization (BiLO) [4] models the DNDP and many other problems in which an agent (the *leader*) makes decisions that minimize their cost function subject to another agent's (the *follower's*) best response. In the DNDP, the *leader* is the transportation planner and the *follower* is the population of drivers, giving rise to the following optimization problem:

$$\begin{aligned}
& \min_{\mathbf{x} \in \{0,1\}^{|A_2|}, \mathbf{y}} && \sum_{(i,j) \in A} t(y_{ij})y_{ij} \\
& \text{s.t.} && \sum_{(i,j) \in A_2} g_{ij}x_{ij} \leq B, \\
& \mathbf{y} \in \arg \min_{\mathbf{y}' \in \mathbb{R}_+^{|A|}} && \sum_{(i,j) \in A} \int_0^{y'_{ij}} t_{ij}(v)dv = \sum_{(i,j) \in A} T_{ij}y'_{ij} + \frac{0.15T_{ij}}{5c_{ij}^4} (y'_{ij})^5 \\
& \text{s.t.} && \mathbf{y}' \text{ is a valid network flow,} \\
& && x_{ij} = 0 \implies y'_{ij} = 0,
\end{aligned}$$

where $A_2 \cap A_1 = \emptyset, A = A_1 \cup A_2$. The leader minimizes the total travel time across all links subject to a budget constraint and the followers' equilibrium which is expressed as a network flow on the graph augmented by the leader's selected edges that satisfies O-D demands; the integral in the follower's objective models the desired equilibrium and evaluates to a degree-5 convex polynomial function in \mathbf{y}' .

Going beyond the DNDP, Dempe [18] lists more than 70 applications of BiLO ranging from pricing in electricity markets (leader is an electricity-supplying retailer that sets the price to maximize profit, followers are consumers who react accordingly to satisfy their demand [61]) to interdiction problems in security settings (leader inspects a budgeted subset of nodes on a road network, follower selects a path such that they evade inspection [58]).

Scope of this work. In this work, we are interested in *mixed-integer non-linear bilevel optimization* problems, simply referred to hereafter as *bilevel optimization* or BiLO, a very general class of bilevel problems where all constraints and objectives may involve non-

linear terms and integer variables. At a high level, we have identified three limitations of existing computational methods for BiLO:

- (i.) The state-of-the-art exact solvers of Fischetti et al. [26] and Tahernejad et al. [56] are limited to mixed-integer bilevel *linear* (MILP) problems and do not scale well. When quick high-quality solutions to large-scale problems are sought after, such exact solvers may be ineffective.
- (ii.) Specialized algorithms, heuristic or exact, do not generalize beyond the single problem they were designed for. For instance, the state-of-the-art exact Knapsack Interdiction solver [59] only works for a single knapsack constraint and fails with two or more, a significant limitation even if one is strictly interested in knapsack-type problems.
- (iii.) Existing methods, exact or heuristic, generic or specialized, are not designed for the “data-driven algorithm design” setting [3] in which similar instances are routinely solved and the goal is to construct generalizable high-efficiency algorithms that leverage historical data.

Contributions. NEUR2BiLO (for *Neural Bilevel Optimization*) is a learning-based framework for bilevel optimization that deals with these issues simultaneously. The following series of observations make NEUR2BiLO possible:

- (i.) **Data collection is “easy”:** For a fixed leader’s decision, the optimal value of the follower can be computed by an appropriate (single-level) solver (e.g., for mixed-integer programming (MIP) or convex programming), enabling the collection of samples of the form (leader’s decision, follower’s value, leader’s value).
- (ii.) **Offline learning in the data-driven setting:** While obtaining data online may be prohibitive, access to historical training instances affords us the ability to construct, offline, a large dataset of samples that can then serve as the basis for learning an approximate value function using supervised regression. The output of this training is a regressor mapping an instance-leader’s decision pair to an estimated follower or leader value.
- (iii.) **MIP embeddings of neural networks:** Should the regressor be MIP-representable, e.g., a feedforward ReLU neural network or a decision tree, it is possible to use a MIP solver to find the leader’s decision that minimizes the regressor’s output. This MIP, which includes any leader constraints, thus serves as an approximate single-level surrogate of the original bilevel problem instance.
- (iv.) **Follower’s constraints via the value function reformulation:** The final ingredient of the NEUR2BiLO recipe is to include any follower’s constraints, some of which may involve leader’s variables. This makes the surrogate problem a heuristic version of the well-known *value function reformulation* (VFR) in BiLO. The VFR transforms a bilevel problem into a single-level one, assuming that one can represent the follower’s value (as a function of the leader’s decision) compactly. This is typically impossible as the

value function may require an exponential number of constraints, a bottleneck that is circumvented by our rather small (approximate) regression models.

- (v.) **Theoretical guarantees:** For interdiction problems, a class of BiLO problems that attracts much attention, NEUR2BiLO solutions have a constant, additive absolute optimality gap which mainly depends on the prediction accuracy of the regression model that approximates the follower’s value function.

Through a series of experiments on (i) the bilevel knapsack interdiction problem, (ii) the “critical node problem” from network security, (iii) a donor-recipient healthcare problem, and (iv) the DNDP, we will show that NEUR2BiLO is easy to train and produces, very quickly, heuristic solutions that are competitive with state-of-the-art methods.

2 Background

Bilevel optimization (BiLO) deals with hierarchical problems where the *leader* (or *upper-level*) problem decides on $\mathbf{x} \in \mathcal{X}$ and parameterizes the *follower* (or *lower-level*) problem that decides on $\mathbf{y} \in \mathcal{Y}$; the sets \mathcal{X} and \mathcal{Y} represent the domains of the variables (continuous, mixed-integer, or pure integer). Both problems have their own objectives and constraints, resulting in the following model:

$$\min_{\mathbf{x} \in \mathcal{X}, \mathbf{y}} F(\mathbf{x}, \mathbf{y}) \tag{1a}$$

$$\text{s.t. } G(\mathbf{x}, \mathbf{y}) \geq \mathbf{0}, \tag{1b}$$

$$\mathbf{y} \in \arg \max_{\mathbf{y}' \in \mathcal{Y}} \{f(\mathbf{x}, \mathbf{y}') : g(\mathbf{x}, \mathbf{y}') \geq \mathbf{0}\}, \tag{1c}$$

where we consider the general mixed-integer non-linear case with $F, f : \mathcal{X} \times \mathcal{Y} \rightarrow \mathbb{R}$, $G : \mathcal{X} \times \mathcal{Y} \rightarrow \mathbb{R}^{m_1}$, and $g : \mathcal{X} \times \mathcal{Y} \rightarrow \mathbb{R}^{m_2}$ non-linear functions of the upper-level \mathbf{x} and lower-level variables \mathbf{y} .

The applicability of exact (i.e., global) approaches severely depends on the nature of the lower-level problem. In case of a continuous lower-level problem which admits strong duality the Karush-Kuhn-Tucker (KKT) conditions can be used to reformulate the bilevel problem into a single-level problem. Solving a BiLO problem with integers in the lower level necessitates more sophisticated methods such as branch and cut [19, 26] along with some assumptions; DeNegre and Ralphs [19] do not allow for coupling constraints (i.e., $G(\mathbf{x}, \mathbf{y}) = G(\mathbf{x})$), and both methods do not allow for continuous upper-level variables to appear in the lower-level constraints $g(\mathbf{x}, \mathbf{y})$. Other approaches such as Benders decomposition [27] are also applicable. Gümüş and Floudas [31] propose single-level reformulations of mixed-integer non-linear BiLO problems to single-level problems using polyhedral theory, an approach that only works for small problems. Later, “branch-and-sandwich” methods were proposed [35, 48] where bounds on both levels’ value functions are used to get an optimal solution. The methods for non-linear BiLO generally do not scale well. We refer to Kleinert et al. [34] for a survey of exact methods for BiLO.

Assumptions. In this work, we make the following standard assumptions:

1. One or both of the following assumptions are met:
 - (a) The follower’s problem has a feasible solution for each $\mathbf{x} \in \mathcal{X}$;
 - (b) There are no coupling constraints in the leader’s problem, i.e., $G(\mathbf{x}, \mathbf{y}) = G(\mathbf{x})$.
2. The optimal follower value is always attained by a feasible solution [see 5, Section 7.2].

Value function reformulation. We consider the so-called *optimistic* setting: if the follower has multiple optima for a given leader’s decision, the one that optimizes the leader’s objective is implemented. We can then rewrite problem (1) using the *value function reformulation* (VFR):

$$\min_{\mathbf{x} \in \mathcal{X}, \mathbf{y} \in \mathcal{Y}} F(\mathbf{x}, \mathbf{y}) \tag{2a}$$

$$\text{s.t. } G(\mathbf{x}, \mathbf{y}) \geq \mathbf{0}, \tag{2b}$$

$$g(\mathbf{x}, \mathbf{y}) \geq \mathbf{0}, \tag{2c}$$

$$f(\mathbf{x}, \mathbf{y}) \geq \Phi(\mathbf{x}), \tag{2d}$$

with the *optimal lower-level value function* defined as

$$\Phi(\mathbf{x}) = \max_{\mathbf{y} \in \mathcal{Y}} \{f(\mathbf{x}, \mathbf{y}) : g(\mathbf{x}, \mathbf{y}) \geq \mathbf{0}\}. \tag{3}$$

Lozano and Smith [42] used this formulation to construct an exact algorithm (without any public code) for solving mixed-integer non-linear BiLO problems with purely integer upper-level variables. Sinha et al. [53, 54, 55] have proposed a family of evolutionary heuristics for continuous non-linear BiLO problems that approximate the optimal value function by using quadratic and Kriging (i.e., a function interpolation method) approximations. Taking it one step further, Beykal et al. [10] extends the framework of the previous authors to handle mixed-integer variables in the lower level.

3 Related Work

3.1 Bilevel optimization

Besides the exact algorithms described in Section 2, there are many heuristics for BiLO as surveyed recently by Camacho-Vallejo et al. [11]. The authors conclude that population-based [7] approaches are the most commonly used meta-heuristics. Generally, these methods are not equipped to deal with hard constraints and therefore do not apply to combinatorial optimization without extensive specialization.

Besides the approximation-based VFR approaches of Sinha et al. [53, 54, 55] and Beykal et al. [10] discussed in Section 2, other learning-based methods have been introduced to solve BiLO problems. Bagloee et al. [2] present a heuristic for DNDP which

uses a linear prediction of the leader’s objective function. The authors propose an iterative algorithm that updates the prediction with new solutions and terminates after a pre-determined number of iterations. Chan et al. [15] propose to simultaneously optimize the parameters of a learning model for a subset of followers in a large-scale cycling network design problem. Here, only non-parametric or linear models are utilized as optimizing more sophisticated learning models is generally challenging with MILP-based optimization.

Molan and Schmidt [45] make use of a neural network to predict the follower variables. The authors assume a setting with a black-box follower’s problem, a leader with a single decision variable, and no coupling constraints. The trained neural network is embedded in a single-level reformulation using a Lipschitz decomposition of the learned neural network. Another learning-based heuristic is proposed by Kwon et al. [38] for a bilevel knapsack problem. Their method uses a graph neural network to obtain the distribution from which to sample the leader’s decisions. This approach is tailored to knapsack and requires a sophisticated, GPU-based, problem-specific architecture for which no code is publicly available.

For continuous unconstrained bilevel optimization, many methods have been proposed recently due to interest in solving nested problems in machine learning (hyperparameter tuning, meta-learning, etc.) [40]. State-of-the-art methods such as Kwon et al. [37] should be used in such continuous unconstrained settings which are orthogonal to our interest in mixed-integer constrained problems.

3.2 Data-driven optimization

The integration of a trained machine learning model into a MIP is a vital element of NEUR2BiLO. This is possible due to MILP formulations of neural networks [16, 24, 52], and of other predictors like decision trees [9, 41]. These methods have become easily applicable due to open software implementations [8, 14, 43] and the `gurobi-machinelearning` library¹ which can automatically generate variables and constraints to represent various trained linear, neural network, and decision tree models from machine learning libraries. One such application is constraint learning when the constraints are unknown [23].

More similar to our setting are the approaches in [21, 22, 36] for predicting value functions of other nested problems such as two-stage stochastic and robust optimization. Our method caters to the specificities of BiLO, particularly in the lower-level approximation (Section 4.2) which leverages the VFR and performs well in highly-constrained BiLO settings such as the DNDP, has approximation guarantees based on the error of the predictive model, and computational results on problems with non-linear interactions between the variables in each stage of the optimization problem; these aspects distinguish NEUR2BiLO from prior work.

¹<https://gurobi-machinelearning.readthedocs.io/en/stable/>

4 Methodology

NEUR2BILO refers to two learning-based single-level reformulations for general BiLO problems. The reformulations rely on representing the thorny nested structure of a BiLO problem with a trained regression model that predicts either the upper-level or lower-level value function.

4.1 Upper-level approximation

The obvious bottleneck in solving BiLO problems is their nested structure. One rather straightforward way of circumventing this difficulty is to get rid of the lower level altogether in the formulation, but predict its optimal value. Namely, we predict the optimal upper-level objective value function as follows

$$\text{NN}^u(\mathbf{x}; \Theta) \approx F(\mathbf{x}, \mathbf{y}^*), \quad (4)$$

where Θ are the weights of a neural network, F the objective function of the leader (2b), and \mathbf{y}^* an optimal solution to the lower level problem (3). To train such a model, one can sample \mathbf{x} from \mathcal{X} , solve (3) to obtain an optimal lower-level solution \mathbf{y}^* , and subsequently compute a label $F(\mathbf{x}, \mathbf{y}^*)$. Under Assumption 1(b), we can then model the single-level problem as

$$\min_{\mathbf{x} \in \mathcal{X}} \text{NN}^u(\mathbf{x}; \Theta) \quad \text{s.t.} \quad G(\mathbf{x}) \geq \mathbf{0}, \quad (5)$$

where we only optimize for \mathbf{x} and thus dismiss the lower-level constraints and objective function. A trained feedforward neural network $\text{NN}^u(\cdot; \Theta)$ with ReLU activations can be represented as a mixed-integer linear program (MILP) [24], where now the input (and output) of the network are decision variables. With this representation, Problem (5) becomes a single-level problem and can be solved using an off-the-shelf MIP solver. Note that linear and decision tree-based models also admit MILP representations [41].

This reformulation is similar to the approach by Bagloee et al. [2], wherein the upper-level value function is predicted using linear regression. Our method differs in that it is not iterative and does not require the use of “no-good cuts” (which avoid reappearing solutions \mathbf{y}). As such, our method is extremely efficient as will be shown experimentally.

The formulation of (5) only allows for problem classes that do not have coupling constraints, i.e., $G(\mathbf{x}, \mathbf{y}) = G(\mathbf{x})$ (Assumption 1(b)). Moreover, the feasibility of a solution \mathbf{x} in the original BiLO problem is not guaranteed unless Assumption 1(a) is also satisfied, an issue that will be addressed in Section 4.3.

4.2 Lower-level approximation

This variant of NEUR2BILO makes use of the VFR (2). The VFR moves the nested complexity of a BiLO to constraint (2d), where the right-hand side is the optimal value of the lower-level problem, parameterized by \mathbf{x} . In practice, enforcing (2d) may require an exponential number of constraints, making it impossible to implement directly. Instead, we

introduce a learning-based VFR in which $\Phi(\mathbf{x})$ is approximated by a regression model with parameters Θ :

$$\text{NN}^l(\mathbf{x}; \Theta) \approx \Phi(\mathbf{x}). \quad (6)$$

Both NN^l and NN^u take in a leader's decision as input and require solving the follower (3) for data generation. By replacing $\Phi(\mathbf{x})$ with $\text{NN}^l(\mathbf{x}; \Theta)$ in (2d) and introducing a slack variable $s \in \mathbb{R}_+$, the surrogate VFR reads as:

$$\min_{\substack{\mathbf{x} \in \mathcal{X}, \mathbf{y} \in \mathcal{Y} \\ s \geq 0}} F(\mathbf{x}, \mathbf{y}) + \lambda s \quad (7a)$$

$$\text{s.t. } G(\mathbf{x}, \mathbf{y}) \geq \mathbf{0}, \quad (7b)$$

$$g(\mathbf{x}, \mathbf{y}) \geq \mathbf{0}, \quad (7c)$$

$$f(\mathbf{x}, \mathbf{y}) \geq \text{NN}^l(\mathbf{x}; \Theta) - s. \quad (7d)$$

All follower and leader constraints of the original BiLO problem are part of Problem (7). However, without the slack variable, i.e., with $s = 0$, the problem could become infeasible due to inaccurate predictions of the neural network. This happens when $\text{NN}^l(\mathbf{x}; \Theta)$ strictly overestimates the follower's optimal value for each \mathbf{x} . In this case, there does not exist a follower decision for which constraint (7d) is satisfied. A value of $s > 0$ can be used to make constraint (7d) satisfiable at a cost of λs in the objective, guaranteeing feasibility.

4.3 Bilevel feasibility

Given a solution \mathbf{x}^* or a solution pair $(\mathbf{x}^*, \tilde{\mathbf{y}})$ returned by our upper- or lower-level approximations, respectively, we would like to produce a lower-level solution \mathbf{y}^* such that $(\mathbf{x}^*, \mathbf{y}^*)$ is bilevel-feasible, i.e., it satisfies the original BiLO in (1), or a certificate of infeasibility of \mathbf{x}^* . The following procedure achieves this goal:

1. Compute the follower's optimal value under \mathbf{x}^* , i.e., $\Phi(\mathbf{x}^*)$, by solving (3).
2. Compute a bilevel-feasible follower solution \mathbf{y}^* by solving problem (2) with fixed \mathbf{x}^* and the right-hand side of (2d) set to $\Phi(\mathbf{x}^*)$, a constant. Return $(\mathbf{x}^*, \mathbf{y}^*)$.

If only Assumption 1(a) is satisfied, then only the lower-level approximation is applicable and this procedure guarantees an optimistic bilevel-feasible solution for it. If only Assumption 1(b) is satisfied, then this procedure can detect in Step 1 that an upper-level approximation's solution \mathbf{x}^* does not admit a follower solution, i.e., that it is infeasible, or calculates a feasible \mathbf{y}^* if one exists in Step 2. If both Assumptions 1(a) and 1(b) are satisfied simultaneously, then this procedure guarantees an optimistic bilevel-feasible solution for either approximation. Proofs of these claims are provided in Appendix A.

4.4 Upper- v.s. lower-level approximation

Generality. The following example shows that under Assumption 1(b), it may happen that (5) returns an infeasible solution while (7) does not. Consider the problem

$$\begin{aligned} \min_{x \in \{0,1\}} \quad & y \\ \text{s.t.} \quad & y \in \arg \max_{y \in \{0,1\}} \{y : 2x + y \leq 1\}. \end{aligned}$$

Solution $x = 1$ makes the follower’s problem infeasible. For solution $x = 0$, the optimal follower solution is $y = 1$ leading to the optimal value 1. Assume that the same trained neural network is used in both approaches; this is possible since leader and follower have the same objective functions. If it predicts $\text{NN}(0) = 2$ and $\text{NN}(1) = 0$, then the upper-level approximation problem (5) will return $x = 1$ which is infeasible whereas the lower-level approximation (7) correctly returns $x = 0$.

Scalability. The upper-level approximation has fewer variables and constraints than its lower-level counterpart as it does not represent the follower’s problem directly. For problems such as the DNDP in which the lower-level problem is large, e.g., necessitating constraints for each node and link to enforce a network flow in the follower solution, this property makes the upper-level approximation easier to solve, possibly at a sacrifice in final solution quality. This trade-off will be assessed experimentally.

4.5 Learning architecture

In previous sections, for ease of notation, all regression models consider the input to be the upper-level decision variables. However, in our experiments, we leverage instance information as well to train a single model that can be deployed on a family of instances. This is done by leveraging information such as coefficients in the objective and constraints for each problem. More details on the specific instance features for each problem are described in Appendix D.1.

For the model’s architecture, our design philosophy consists of first explicitly representing or learning instance-based features, then combining instance-based features with (leader) decision variable information to make predictions. For problems wherein instance-based features are learned, we use a set-based architecture akin to DeepSets [60] but note that this can also be done via a feedforward or graph neural network depending on the problem structure. NEUR2BILO is largely agnostic to the learning model utilized as long as it is MILP-representable. In our experiments, we primarily focus on neural networks, but for some problems also explore the use of gradient-boosted trees (GBT).

The overall architecture can be summarized as the following set of operations. Fix a particular instance of a BiLO problem and let n be the number of leader variables, \mathbf{f}_i a vector of features for each leader variable \mathbf{x}_i (independently of the variable’s value), and $h(\mathbf{x}_i)$ a feature map that describes the i th leader variable for a specific value of that variable. The functions Ψ^s , Ψ^d , and Ψ^v are neural networks with appropriate input-output dimensions; the functions SUM, CONCAT, and AGGREGATE sum up a set of vectors, concatenate two

vectors into a single column vector, and aggregate a set of scalar values (e.g., by another neural network or simply summing them up), respectively. Our final value predictions are derived by:

- (i.) Embedding the set of variable features $\{\mathbf{f}_i\}$ using a set-based architecture, e.g., the same network Ψ^d , summing up the resulting n variable embeddings, then passing the resulting vector to network Ψ^s , yielding a vector we refer to as the INSTANCEEMBEDDING:

$$\text{INSTANCEEMBEDDING} = \Psi^s(\text{SUM}(\{\Psi^d(\mathbf{f}_i)\}_{i=1}^n)).$$

This is akin to the DeepSets approach of Zaheer et al. [60].

- (ii.) Conditional on a specific assignment of values to the leader’s decision vector \mathbf{x} , a per-variable embedding is computed by network Ψ^v to allow for interactions between the INSTANCEEMBEDDING and the specific assignment of variable i as represented by $h(\mathbf{x}_i)$:

$$\text{VARIABLEEMBEDDING}(i) = \Psi^v(\text{CONCAT}(h(\mathbf{x}_i), \text{INSTANCEEMBEDDING})).$$

- (iii.) The final value prediction for either of our approximations aggregates the variable embeddings possibly after passing them through a function g_i :

$$\text{NN}(\mathbf{x}; \Theta) = \text{AGGREGATE}(\{g_i(\text{VARIABLEEMBEDDING}(i))\}_{i=1}^n).$$

For example, if the follower’s objective is a linear function and VARIABLEEMBEDDING(i) is a scalar, then it is useful to use the variable’s known objective function coefficient d_i here, i.e.: $g_i(\text{VARIABLEEMBEDDING}(i)) = d_i \cdot \text{VARIABLEEMBEDDING}(i)$. The final step is to aggregate the per-variable $g_i(\cdot)$ outputs, e.g., by a summation for linear or separable objective functions.

The vector Θ includes all learnable parameters of networks Ψ^s , Ψ^d , and Ψ^v . More details on the specific architectures for each problem can be found in Appendix D.1.

4.6 Approximation guarantees

4.6.1 Lower-level approximation

In this section we consider the lower-level approximation with $\text{NN}^l(\mathbf{x}; \Theta)$. All proofs are deferred to Appendix B.

Since the prediction of the neural network is only an approximation of the true optimal value of the follower’s problem $\Phi(\mathbf{x})$, NEUR2BILO may return sub-optimal solutions for the original problem (1). In this section, we derive approximation guarantees for a specific setup.

Let it be that Assumption 1(a) holds and that the neural network approximates the optimal value of the follower’s problem up to an absolute error of $\alpha > 0$, i.e.,

$$|\text{NN}^l(\mathbf{x}; \Theta) - \Phi(\mathbf{x})| \leq \alpha \quad \text{for all } \mathbf{x} \in \mathcal{X}. \tag{8}$$

We consider the special case where the leader and the follower have the same objective function, i.e., $f(\mathbf{x}, \mathbf{y}) = F(\mathbf{x}, \mathbf{y})$ for all $\mathbf{x} \in \mathcal{X}, \mathbf{y} \in \mathcal{Y}$. We furthermore define the parameter Δ as the maximum difference of functions values $f(\mathbf{x}, \mathbf{y}) - f(\mathbf{x}, \mathbf{y}') \geq 0$ over all $\mathbf{x} \in \mathcal{X}, \mathbf{y}, \mathbf{y}' \in \mathcal{Y}$ such that no $\tilde{\mathbf{y}} \in \mathcal{Y}$ exists which has function value $f(\mathbf{x}, \mathbf{y}) > f(\mathbf{x}, \tilde{\mathbf{y}}) > f(\mathbf{x}, \mathbf{y}')$. Note that Δ can be strictly larger than zero if the follower decisions are integer.

For a fixed $\mathbf{x} \in \mathcal{X}$, $\mathbf{y}_{\text{NN}}^*(\mathbf{x})$ denotes an optimal solution of (7). Furthermore, for any given $\mathbf{y} \in \mathcal{Y}$ we denote by $s^*(\mathbf{x}, \mathbf{y})$ an optimal slack-value in Problem (7) if the upper- and lower-level variables are fixed to \mathbf{x} and \mathbf{y} , respectively.

Observation 1. For any $\mathbf{x} \in \mathcal{X}$ and $\mathbf{y} \in \mathcal{Y}$ we have

$$s^*(\mathbf{x}, \mathbf{y}) = \max\{0, \text{NN}^l(\mathbf{x}; \Theta) - f(\mathbf{x}, \mathbf{y})\}.$$

Lemma 1. Assume the leader and the follower have the same objective function and $\lambda > 1$. Then, for any given $\mathbf{x} \in \mathcal{X}$ the following conditions hold for the optimal follower solution $\mathbf{y}_{\text{NN}}^*(\mathbf{x})$ of Problem (7):

- If $\text{NN}^l(\mathbf{x}; \Theta) \geq \Phi(\mathbf{x})$, then $f(\mathbf{x}, \mathbf{y}_{\text{NN}}^*(\mathbf{x})) = \Phi(\mathbf{x})$, i.e., $(\mathbf{x}, \mathbf{y}_{\text{NN}}^*(\mathbf{x}))$ is feasible for the original bilevel problem.
- If $\text{NN}^l(\mathbf{x}; \Theta) < \Phi(\mathbf{x})$, then

$$\text{NN}^l(\mathbf{x}; \Theta) - \frac{1}{\lambda}\Delta \leq f(\mathbf{x}, \mathbf{y}_{\text{NN}}^*(\mathbf{x})) \leq \Phi(\mathbf{x}).$$

The latter lemma states that if the neural network overestimates the follower value for a solution $\mathbf{x} \in \mathcal{X}$, then the surrogate problem (7) still selects an optimal follower response. However, if the neural network underestimates the value, the surrogate problem may choose a follower response for which the objective value is either larger than the true value or differs by at most $\frac{1}{\lambda}\Delta$. Note that the latter term can be controlled by increasing the penalty λ .

By applying Lemma 1 we can bound the approximation error of the lower-level NEUR2BILO.

Theorem 1. Let $\lambda > 1$. If the leader and the follower have the same objective function and opt is the optimal value of (1), NEUR2BILO returns a feasible solution $(\mathbf{x}^*, \mathbf{y}^*)$ for Problem (1) with objective value

$$f(\mathbf{x}^*, \mathbf{y}^*) \leq \text{opt} + 3\alpha + \frac{2}{\lambda}\Delta.$$

4.6.2 Upper-level approximation

As the first example in Section 4.4 shows, it may happen that the upper-level surrogate problem (5) returns an infeasible solution and hence no approximation guarantee can be derived in this case. However, in the case where all leader solutions are feasible and the neural network predicts for every $\mathbf{x} \in \mathcal{X}$ an upper-level objective value that deviates at most $\alpha > 0$ from the true one, the returned solution trivially approximates the true optimal value with an absolute error of at most 2α . This follows since the worst that can happen is

Problem		Leader			Follower			Reference	Baseline
		x	Obj.	Cons.	y	Obj.	Cons.		
KIP	($\downarrow\uparrow$)	B	Lin	Lin	B	Lin	Lin	[57]	B&C [26]
CNP	($\uparrow\uparrow$)	B	BLin	Lin	B	BLin	Lin	[13]	B&C [26]
DRP	($\uparrow\uparrow$)	C	Lin	Lin	MI	Lin	BLin	[29]	B&C+ [29]
DNDP	($\downarrow\uparrow$)	B	NLin	Lin	C	NLin	Lin	[50]	MKKT [27]

Table 1: Problem class characteristics. All problems have a single knapsack (budget) constraint in the leader; for the follower, the DNDP has network flow constraints whereas other problems have a knapsack constraint. The arrows refer to minimization (\downarrow) or maximization (\uparrow) in leader and follower, respectively. B = Binary, C = Continuous, MI = Mixed-Integer, Lin = Linear, BLin = Bilinear, NLin = Non-Linear.

that the objective value of the optimal solution is overestimated by α while a solution with objective value $\text{opt} + 2\alpha$ is underestimated by α and hence has the same predicted value as the optimal solution. Problem (5) then may return the latter sub-optimal solution.

5 Experimental Setup

Benchmark problems. The characteristics of the four problems we evaluate on are summarized in Table 1; their MIP formulations are deferred to Appendix C and brief descriptions follow. We note that all four problems satisfy both Assumptions 1(a) and 1(b), making it possible to obtain bilevel-feasible solutions using the procedure of Section 4.3. We will only perform Step 1 as Step 2 is only necessary if there are multiple optima to the follower problem, an unlikely situation given the random objective function coefficients in KIP, CNP, and DRP; the DNDP follower is convex with a unique optimum.

- **Knapsack interdiction (KIP)** [12, 57]: The leader interdicts a subset of at most k items and the follower solves a knapsack problem over the remaining (non-interdicted) items. The leader aims to minimize the follower’s (maximization) objective.
- **Critical node problem (CNP)** [13, 20]: This problem regards the protection (by the leader) of resources in a network against malicious attacks (by the follower), and has applications in the protection of computer networks against cyberattacks as demonstrated by Dragotto et al. [20] on real data from an Ericsson cloud security system. The CNP is a special case of the “critical node game” [20] which is a non-sequential multi-round game that was adapted to the sequential multi-level (and particularly bilevel) setting by Carvalho et al. [13].
- **Donor-recipient problem (DRP)** [46]: This problem relates to the donations given by certain agencies to countries in need of, e.g., healthcare projects. The leader (the donor agency) decides on which proportion of the cost, per project, to subsidize, whereas the follower (a country) decides which projects it implements.

- **Discrete network design problem (DNDP) [50]:** This is the problem described in [Section 1](#). We build on the work of Rey [50] who provided benchmark instances for the transportation network of Sioux Falls, South Dakota, and an implementation of the state-of-the-art method of Fontaine and Minner [27]. This network and corresponding instances are representative of the state of the DNDP in the literature.

Baselines. As previously mentioned, the branch-and-cut (B&C) algorithm by Fischetti et al. [26] is considered to be state-of-the-art for solving mixed-integer linear BiLO. The method is applicable if the continuous variables of the leader do not appear in the follower’s constraints. Both KIP and CNP meet these assumptions. This algorithm will act as the baseline for these problems. For DRP, we compare against the results produced by an algorithm in the branch-and-cut paradigm (B&C+) from Ghatkar et al. [29]. For DNDP, the follower’s problem only has continuous variables, so the baseline is a method based on KKT conditions (MKKT) [27].

Data collection & Training. For each problem class, data is collected by sampling feasible leader decisions \mathbf{x} and then solving $\Phi(\mathbf{x})$ to compute either the upper- or lower-level objectives as labels. We then train regression models to minimize the least-squares error on the training samples. Typically, data collection and training take less than one hour, a negligible cost given that for larger instances baseline methods require more time *per instance*. Additionally, the same trained model can be used on multiple unseen test instances. We report detailed times for data collection and training in [Appendix D.2](#).

Computational setup. The experiments for three out of four benchmarks were run on a computing cluster with an Intel Xeon CPU E5-2683 and Nvidia Tesla P100 GPU with 64GB of RAM (for training). The experiments for one benchmark were run on a virtual machine with two Intel Xeon(R) CPUs at 2.20GHz and 12GB of RAM. Pytorch 2.0.1 [47] was used for all neural network models and scikit-learn 1.4.0 was used for gradient-boosted trees in the DNDP [49]. Gurobi 11.0.1 [32] was used as the MILP solver and `gurobi-machinelearning` 1.4.0 was used to embed the learning models into MILPs. For evaluation in KIP, CNP, and DRP, all solving was limited to 1 hour. For DNDP, we consider a more limited-time regime, wherein we compare NEUR2BiLO to run for 5 seconds against the baseline evaluated at 5, 10, and 30 seconds. For all problems, we evaluate both the lower- and upper-level approximations with neural networks, namely NN^l and NN^u . For DNDP, we additionally include GBT, i.e., GBT^l and GBT^u as the lower- and upper-level approximations with 50 tree estimators. For NN^l and GBT^l we set $\lambda = 1$ for all results presented in the main paper. Our code and data are at <https://github.com/khalil-research/Neur2BiLO>.

6 Experimental Results

We now summarize the results as measured by average solution times and mean relative errors (MREs). The relative error is computed as $100 \cdot \frac{|obj_A - obj_{best}|}{|obj_{best}|}$, where obj_A is objective

n	k	NN ^l		NN ^u		G-VFA		B&C	
		MRE	Time	MRE	Time	MRE	Time	MRE	Time
18	5	1.48	0.59	1.48	0.34	1.82	0.14	0.00	9.55
18	9	1.51	0.59	1.51	0.43	3.97	0.22	0.00	5.81
18	14	0.00	0.22	0.00	0.17	64.22	0.03	0.00	0.39
20	5	0.41	0.62	0.41	0.45	2.19	0.25	0.00	23.18
20	10	0.99	0.66	0.99	0.58	0.99	0.36	0.00	10.27
20	15	3.57	0.32	3.57	0.19	23.39	0.02	0.00	0.94
22	6	0.71	0.19	0.71	0.18	0.42	0.18	0.00	42.30
22	11	1.01	0.28	1.01	0.28	1.08	0.33	0.00	16.26
22	17	14.43	0.24	14.43	0.15	14.43	0.13	0.00	0.68
25	7	0.44	2.66	0.44	2.42	0.44	0.64	0.00	137.96
25	13	1.42	2.75	1.42	2.79	3.85	1.24	0.00	48.43
25	19	2.49	0.48	2.49	0.38	2.49	0.13	0.00	1.77
28	7	0.39	0.67	0.39	0.74	0.26	0.62	0.00	309.18
28	14	0.75	2.10	0.75	1.45	1.37	1.29	0.00	120.74
28	21	1.14	0.45	1.14	0.49	3.16	0.31	0.00	4.92
30	8	0.00	1.54	0.00	1.54	0.43	0.97	0.00	792.44
30	15	0.49	3.64	0.49	3.06	0.75	1.35	0.00	187.23
30	23	2.29	1.08	2.29	0.73	4.48	0.25	0.00	5.65
100	25	0.93	10.02	0.93	8.40	0.00	4.19	8.09	3,600.40
100	50	0.96	51.68	0.96	49.28	0.04	53.74	8.96	3,600.44
100	75	0.08	24.69	0.08	23.78	0.12	35.27	5.87	3,600.52
Avg. $n \leq 30$		1.86	1.06	1.86	0.91	7.21	0.47	0.00	95.43
Avg. $n = 100$		0.66	28.80	0.66	27.15	0.05	31.07	7.64	3,600.45

Table 2: Knapsack Results. n and k denote the number of items and the interdiction budget, respectively. For $n \leq 30$, we directly evaluate on the 180 instances (10 per size) of Tang et al. [57]; each value is the average over 10 instances. For $n = 100$, our evaluation instances (100 per size) are generated using the same procedure of Tang et al. [57]. The no-learning baseline G-VFA is a VFR using the follower’s greedy solution as a lower-level value function approximator. All times in seconds.

$ V $	NN ^l		NN ^u		B&C	
	MRE	Time	MRE	Time	MRE	Time
10	3.20	0.04	2.75	0.02	1.01	4.24
25	2.60	0.23	1.77	0.05	0.73	3,244.20
50	1.42	0.38	0.98	0.10	0.67	3,600.30
100	1.12	0.48	0.56	0.42	1.79	3,600.65
300	2.01	1.12	0.33	0.83	2.32	3,600.54
500	1.33	1.69	0.45	1.19	2.47	3,600.80
Average	1.95	0.66	1.14	0.43	1.50	2,941.79

Table 3: Critical Node Problem Results. $|V|$ denote the number of nodes. Each row averaged over 300 instances that are randomly sampled using the procedure described in Dragotto et al. [20]. All times in seconds.

Instance #	Relative Error (%)			Time		
	NN ^l	NN ^u	B&C+	NN ^l	NN ^u	B&C+
1	42.28	0.00	20.69	0.09	1.44	3,600.09
2	38.44	0.00	27.82	0.12	1.52	3,600.08
3	45.17	0.00	30.13	0.14	2.85	3,600.07
4	33.68	0.00	18.98	0.07	1.68	3,637.23
5	44.51	0.00	27.29	0.10	1.96	3,600.07
6	35.18	0.00	31.09	0.08	2.93	3,600.10
7	43.58	0.00	21.82	0.09	1.58	3,600.14
8	34.37	0.00	26.79	0.09	0.87	3,600.10
9	37.03	0.00	26.80	0.16	4.55	3,600.16
10	38.89	0.00	28.59	0.12	3.57	3,600.10
Average	39.31	0.00	26.00	0.11	2.30	3,603.82

Table 4: DRP objective results. Each row corresponds to a single instance from dataset 15, the most challenging set of instances from Ghatkar et al. [29]. All times in seconds.

# of edges	budget	NN ^l		NN ^u		GBT ^l		GBT ^u		MKKT		
		MRE	Time	MRE	Time	MRE	Time	MRE	Time	MRE-5	MRE-10	MRE-30
10	25%	0.88	2.89	4.97	0.01	1.21	4.02	1.11	0.04	6.08	0.51	0.10
10	50%	0.06	3.20	3.93	0.01	0.09	3.68	3.70	0.05	7.39	2.17	0.00
10	75%	0.13	2.15	1.49	0.01	0.24	2.21	2.00	0.03	5.88	0.05	0.06
20	25%	1.16	5.01	7.91	0.04	2.17	5.01	5.21	0.26	13.52	6.84	1.33
20	50%	1.45	5.01	4.30	0.05	1.02	5.00	2.65	0.15	16.39	9.02	0.84
20	75%	0.14	2.48	4.87	0.01	0.08	3.53	0.84	0.10	11.02	4.07	0.08
Average		0.64	3.46	4.58	0.02	0.80	3.91	2.58	0.11	10.05	3.78	0.40

Table 5: Discrete Network Design Problem results. Each value is an average across 10 instances from Rey [50]. The budget is a fraction of the total cost of all 30 possible candidate links; see Appendix D.2 for more details. All times in seconds

found from method \mathcal{A} and obj_{best} is the best-known objective found by any of the methods. These results are reported in Tables 2-5. More detailed results that include absolute objective values are in Appendix F and box-plots of the distributions of relative errors are in Appendix G. Our experimental design answers the following questions:

Q1: Can NEUR2BILO find high-quality solutions quickly on classical interdiction problems? Table 2 compares NEUR2BILO to the B&C algorithm of Fischetti et al. [26]. NEUR2BILO terminates in 1-2% of the time required by B&C on the smaller ($n \leq 30$) well-studied KIP instances of Tang et al. [57]. However, when the instance size increases to $n = 100$, both NN^l and NN^u find much better solutions than NEUR2BILO in roughly 30 seconds, even when B&C runs for the full hour. Furthermore, Table 11 in Appendix F shows that B&C requires 10 to 1,000 \times more time than NN^l or NN^u to find equally good solutions. In addition, the best solutions found by B&C at the termination times of NN^l or NN^u are generally worse, even for small instances.

Q2: Do these computational results extend to non-linear and more challenging BiLO problems? Interdiction problems such as the KIP are well-studied but are only a small subset of BiLO. We will shift attention to the more practical problems, starting with the CNP (Table 3). CNP includes terms that are bilinear (i.e., $z = xy$) in the upper- and lower-level variables, resulting in a much more challenging problem for general-purpose B&C. In this case, both NN^l and NN^u tend to outperform B&C as the problem size increases. In addition, the results on incumbents reported in Table 12 in Appendix F are as good, if not even stronger than those of KIP.

Secondly, we discuss DRP (Table 4), where we evaluate on the most challenging instances from Ghahtarani et al. [28], all of which have gaps of $\sim 50\%$ at a 1-hour time limit with B&C+, a specialized B&C-based algorithm. Here NN^u performs remarkably well: it finds the best-known solutions on every single instance in roughly ~ 0.1 seconds at an average improvement in solution quality of 26% over B&C+.

Q3: How does NEUR2BiLO perform on BiLO problems with challenging constraints?

Given that NEUR2BiLO has strong performance on benchmarks with budget constraints, the next obvious question is whether it can be applied to BiLO problems that have complex constraints. To answer this, we will refer to the results in Table 5 for the DNDP. In this setting, we focus on a limited-time regime wherein we compare NEUR2BiLO with a 5-second time limit to MKKT at time limits 5, 10, and 30 seconds. NN^u can achieve high-quality solutions much faster than any other method with only a minor sacrifice in solution quality, making it a great candidate for domains where interactive decision-making is needed (e.g., what-if analysis of various candidate roads, budgets, or origin-destination demand models).

NN^l , on the other hand, takes longer than NN^u but computes solutions that are competitive with the baseline when it runs at least $6\times$ longer. We suspect that the better solution quality from NN^l is due to its explicit modeling of feasible lower-level decisions that “align” with the predictions, whereas NN^u may simply extrapolate poorly. In terms of computing time, one computational burden for NN^l is the requirement to model the non-linear upper- and lower-level objectives, which requires a piece-wise linear approximation based on Fontaine and Minner [27], a step that introduces additional variables and constraints. In addition, the DNDP results include results for GBT^l and GBT^u , demonstrating that other learning models, such as GBT, are directly applicable, and in some cases may even lead to better solution quality, faster optimization, and simpler implementation.

Q4: Can approximations derived from heuristics be useful? We now refer back to KIP and focus on the greedy value function approximation (G-VFA), a KIP-specific approximation that relies on the fact that greedy algorithms are typically good for 1-dimensional knapsack problems. Namely, the heuristic is based on ordering the items with their value-to-weight ratio [17] and is used as the knapsack solution in the follower problem, while still being parameterized by x . This heuristic is embedded in a single-level problem as this heuristic is MILP-representable [1]; we note that we are not aware of uses in the literature of this approximation and it may be of independent interest.

Generally, G-VFA performs quite well, and in some cases outperforms NN^l and NN^u , but there are clear cases where NN^l and NN^u outperform G-VFA demonstrating that learning is beneficial. In addition, heuristics like G-VFA can be utilized to compute features for NN^l and NN^u . For KIP, the inclusion of these features derived from G-VFA strongly improves the results (see Table 10 in Appendix E.3). This demonstrates that there is value in leveraging any problem-specific MILP-representable heuristics as features for learning.

Q5: How does λ affect NN^l ? Table 9 in Appendix E.2 shows that a slack penalty of $\lambda = 0.1$ notably improves the performance of both NN^l and GBT^l for DNDP, compared to the $\lambda = 1$ reported in Table 5. As an alternative to adding slack, one can even dampen predictions of the value function to allow more flexibility using the empirical error observed during training; see Table 8 in Appendix E.1.

7 Conclusion

In both its upper- and lower-level instantiations, NEUR2BILO finds high-quality solutions in a few milliseconds to a few seconds across four benchmarks that span applications in interdiction, network security, healthcare, and transportation planning. In fact, we are not aware of any bilevel optimization method which has been evaluated across such a diverse range of problems as existing methods make stricter assumptions that limit their applicability. NEUR2BILO models are generic, easy to train, and accommodating of problem-specific heuristics as features. Of future interest are potential extensions to bilevel *stochastic* optimization [6], robust optimization with decision-dependent uncertainty [30] (a special case of BiLO), and multi-level problems beyond two levels, e.g. [39].

References

- [1] David Avis, David Bremner, Hans Raj Tiwary, and Osamu Watanabe. Polynomial size linear programs for problems in p . *Discrete Applied Mathematics*, 265:22–39, 2019.
- [2] Saeed Asadi Bagloee, Mohsen Asadi, Majid Sarvi, and Michael Patriksson. A hybrid machine-learning and optimization method to solve bi-level problems. *Expert Systems with Applications*, 95:142–152, 2018.
- [3] Maria-Florina Balcan. Data-driven algorithm design. *arXiv preprint arXiv:2011.07177*, 2020.
- [4] Jonathan F Bard. *Practical bilevel optimization: algorithms and applications*, volume 30. Springer Science & Business Media, 2013.
- [5] Yasmine Beck and Martin Schmidt. A gentle and incomplete introduction to bilevel optimization. *Lecture notes*, 2021.
- [6] Yasmine Beck, Ivana Ljubić, and Martin Schmidt. A survey on bilevel optimization under uncertainty. *European Journal of Operational Research*, 2023.
- [7] Zahra Beheshti and Siti Mariyam Hj Shamsuddin. A review of population-based meta-heuristic algorithms. *Int. j. adv. soft comput. appl*, 5(1):1–35, 2013.
- [8] David Bergman, Teng Huang, Philip Brooks, Andrea Lodi, and Arvind U Raghunathan. JANOS: an integrated predictive and prescriptive modeling framework. *INFORMS Journal on Computing*, 34(2):807–816, 2022.
- [9] Dimitris Bertsimas, Jack Dunn, and Yuchen Wang. Near-optimal nonlinear regression trees. *Operations Research Letters*, 49(2):201–206, 2021.
- [10] Burcu Beykal, Styliani Avraamidou, Ioannis PE Pistikopoulos, Melis Onel, and Efstratios N Pistikopoulos. Domino: Data-driven optimization of bi-level mixed-integer nonlinear problems. *Journal of Global Optimization*, 78:1–36, 2020.

- [11] José-Fernando Camacho-Vallejo, Carlos Corpus, and Juan G Villegas. Metaheuristics for bilevel optimization: A comprehensive review. *Computers & Operations Research*, page 106410, 2023.
- [12] Alberto Caprara, Margarida Carvalho, Andrea Lodi, and Gerhard J Woeginger. Bilevel knapsack with interdiction constraints. *INFORMS Journal on Computing*, 28(2):319–333, 2016.
- [13] Margarida Carvalho, Gabriele Dragotto, Andrea Lodi, and Sriram Sankaranarayanan. Integer programming games: a gentle computational overview. In *Tutorials in Operations Research: Advancing the Frontiers of OR/MS: From Methodologies to Applications*, pages 31–51. INFORMS, 2023.
- [14] Francesco Ceccon, Jordan Jalving, Joshua Haddad, Alexander Thebelt, Calvin Tsay, Carl D Laird, and Ruth Misener. OMLT: Optimization & machine learning toolkit. *arXiv preprint arXiv:2202.02414*, 2022.
- [15] Timothy CY Chan, Bo Lin, and Shoshanna Saxe. A machine learning approach to solving large bilevel and stochastic programs: Application to cycling network design. *arXiv preprint arXiv:2209.09404*, 2022.
- [16] Chih-Hong Cheng, Georg Nührenberg, and Harald Ruess. Maximum resilience of artificial neural networks. In *International Symposium on Automated Technology for Verification and Analysis*, pages 251–268. Springer, 2017.
- [17] George B Dantzig. Discrete-variable extremum problems. *Operations research*, 5(2): 266–288, 1957.
- [18] Stephan Dempe. Bilevel optimization: theory, algorithms, applications and a bibliography. *Bilevel Optimization: Advances and Next Challenges*, pages 581–672, 2020.
- [19] Scott T DeNegre and Ted K Ralphs. A branch-and-cut algorithm for integer bilevel linear programs. In *Operations research and cyber-infrastructure*, pages 65–78. Springer, 2009.
- [20] Gabriele Dragotto, Amine Boukhtouta, Andrea Lodi, and Mehdi Taobane. The critical node game, 2023.
- [21] Justin Dumouchelle, Rahul Patel, Elias B Khalil, and Merve Bodur. Neur2SP: Neural two-stage stochastic programming. *Advances in Neural Information Processing Systems*, 35, 2022.
- [22] Justin Dumouchelle, Esther Julien, Jannis Kurtz, and Elias B Khalil. Neur2ro: Neural two-stage robust optimization. *arXiv preprint arXiv:2310.04345*, 2023.
- [23] Adejuyigbe O Fajemisin, Donato Maragno, and Dick den Hertog. Optimization with constraint learning: a framework and survey. *European Journal of Operational Research*, 2023.

- [24] Matteo Fischetti and Jason Jo. Deep neural networks and mixed integer linear optimization. *Constraints*, 23(3):296–309, 2018.
- [25] Matteo Fischetti, Ivana Ljubić, Michele Monaci, and Markus Sinnl. Intersection cuts for bilevel optimization. In *Integer Programming and Combinatorial Optimization: 18th International Conference, IPCO 2016, Liège, Belgium, June 1-3, 2016, Proceedings 18*, pages 77–88. Springer, 2016.
- [26] Matteo Fischetti, Ivana Ljubić, Michele Monaci, and Markus Sinnl. A new general-purpose algorithm for mixed-integer bilevel linear programs. *Operations Research*, 65(6):1615–1637, 2017.
- [27] Pirmin Fontaine and Stefan Minner. Benders decomposition for discrete–continuous linear bilevel problems with application to traffic network design. *Transportation Research Part B: Methodological*, 70:163–172, 2014.
- [28] Alireza Ghahtarani, Ahmed Saif, Alireza Ghasemi, and Erick Delage. A double-oracle, logic-based benders decomposition approach to solve the k-adaptability problem. *Computers & Operations Research*, 155:106243, 2023.
- [29] Shraddha Ghatkar, Ashwin Arulselman, and Alec Morton. Solution techniques for bi-level knapsack problems. *Computers & Operations Research*, 159:106343, 2023.
- [30] Marc Goerigk, Jannis Kurtz, Martin Schmidt, and Johannes Thürauf. Connections and reformulations between robust and bilevel optimization. *optimization-online preprint*, 2023.
- [31] Zeynep H Gümüş and Christodoulos A Floudas. Global optimization of mixed-integer bilevel programming problems. *Computational Management Science*, 2:181–212, 2005.
- [32] Gurobi Optimization, LLC. Gurobi Optimizer Reference Manual, 2023. URL <https://www.gurobi.com>.
- [33] Diederik P Kingma and Jimmy Ba. Adam: A method for stochastic optimization. *arXiv preprint arXiv:1412.6980*, 2014.
- [34] Thomas Kleinert, Martine Labbé, Ivana Ljubić, and Martin Schmidt. A survey on mixed-integer programming techniques in bilevel optimization. *EURO Journal on Computational Optimization*, 9:100007, 2021.
- [35] Polyxeni-M Kleniati and Claire S Adjiman. A generalization of the branch-and-sandwich algorithm: from continuous to mixed-integer nonlinear bilevel problems. *Computers & Chemical Engineering*, 72:373–386, 2015.
- [36] Jan Kronqvist, Boda Li, Jan Rolfes, and Shudian Zhao. Alternating mixed-integer programming and neural network training for approximating stochastic two-stage problems. *arXiv preprint arXiv:2305.06785*, 2023.

- [37] Jeongyeol Kwon, Dohyun Kwon, Stephen Wright, and Robert D Nowak. A fully first-order method for stochastic bilevel optimization. In *International Conference on Machine Learning*, pages 18083–18113. PMLR, 2023.
- [38] Sunhyeon Kwon, Hwayong Choi, and Sungsoo Park. Solving bilevel knapsack problem using graph neural networks. *arXiv preprint arXiv:2211.13436*, 2022.
- [39] Markus Leitner, Ivana Ljubić, Michele Monaci, Markus Sinnl, and Kübra Tanınmış. An exact method for binary fortification games. *European Journal of Operational Research*, 307(3):1026–1039, 2023.
- [40] Risheng Liu, Jiaxin Gao, Jin Zhang, Deyu Meng, and Zhouchen Lin. Investigating bi-level optimization for learning and vision from a unified perspective: A survey and beyond. *IEEE Transactions on Pattern Analysis and Machine Intelligence*, 44(12):10045–10067, 2021.
- [41] Michele Lombardi, Michela Milano, and Andrea Bartolini. Empirical decision model learning. *Artificial Intelligence*, 244:343–367, 2017.
- [42] Leonardo Lozano and J Cole Smith. A value-function-based exact approach for the bilevel mixed-integer programming problem. *Operations Research*, 65(3):768–786, 2017.
- [43] Donato Maragno, Holly Wiberg, Dimitris Bertsimas, Ş İlker Birbil, Dick den Hertog, and Adejuyigbe O Fajemisin. Mixed-integer optimization with constraint learning. *Operations Research*, 2023.
- [44] Tom V Mathew and KV Krishna Rao. Introduction to transportation engineering, traffic assignment. *Lecture notes*, 2006.
- [45] Ioana Molan and Martin Schmidt. Using neural networks to solve linear bilevel problems with unknown lower level. *Optimization Letters*, pages 1–21, 2023.
- [46] Alec Morton, Ashwin Arulsevan, and Ranjeeta Thomas. Allocation rules for global donors. *Journal of health economics*, 58:67–75, 2018.
- [47] Adam Paszke, Sam Gross, Francisco Massa, Adam Lerer, James Bradbury, Gregory Chanan, Trevor Killeen, Zeming Lin, Natalia Gimelshein, Luca Antiga, Alban Desmaison, Andreas Kopf, Edward Yang, Zachary DeVito, Martin Raison, Alykhan Tejani, Sasank Chilamkurthy, Benoit Steiner, Lu Fang, Junjie Bai, and Soumith Chintala. PyTorch: An imperative style, high-performance deep learning library. In H. Wallach, H. Larochelle, A. Beygelzimer, F. d'Alché-Buc, E. Fox, and R. Garnett, editors, *Advances in Neural Information Processing Systems 32*, pages 8024–8035. Curran Associates, Inc., 2019. <http://papers.neurips.cc/paper/9015-pytorch-an-imperative-style-high-performance-deep-learning-library.pdf>.
- [48] Remigijus Paulavičius and Claire S Adjiman. New bounding schemes and algorithmic options for the branch-and-sandwich algorithm. *Journal of Global Optimization*, 77(2):197–225, 2020.

- [49] F. Pedregosa, G. Varoquaux, A. Gramfort, V. Michel, B. Thirion, O. Grisel, M. Blondel, P. Prettenhofer, R. Weiss, V. Dubourg, J. Vanderplas, A. Passos, D. Cournapeau, M. Brucher, M. Perrot, and E. Duchesnay. Scikit-learn: Machine learning in Python. *Journal of Machine Learning Research*, 12:2825–2830, 2011.
- [50] David Rey. Computational benchmarking of exact methods for the bilevel discrete network design problem. *Transportation Research Procedia*, 47:11–18, 2020.
- [51] David Rey. *Optimization and game-theoretical methods for transportation systems*. PhD thesis, Toulouse 3 Paul Sabatier, 2023.
- [52] Thiago Serra, Christian Tjandraatmadja, and Srikumar Ramalingam. Bounding and counting linear regions of deep neural networks. In *International Conference on Machine Learning*, pages 4558–4566. PMLR, 2018.
- [53] Ankur Sinha, Pekka Malo, and Kalyanmoy Deb. Solving optimistic bilevel programs by iteratively approximating lower level optimal value function. In *2016 IEEE Congress on Evolutionary Computation (CEC)*, pages 1877–1884. IEEE, 2016.
- [54] Ankur Sinha, Zhichao Lu, Kalyanmoy Deb, and Pekka Malo. Bilevel optimization based on iterative approximation of multiple mappings, 2017.
- [55] Ankur Sinha, Samish Bedi, and Kalyanmoy Deb. Bilevel optimization based on kriging approximations of lower level optimal value function. In *2018 IEEE congress on evolutionary computation (CEC)*, pages 1–8. IEEE, 2018.
- [56] Sahar Tahernejad, Ted K Ralphs, and Scott T DeNegre. A branch-and-cut algorithm for mixed integer bilevel linear optimization problems and its implementation. *Mathematical Programming Computation*, 12:529–568, 2020.
- [57] Yen Tang, Jean-Philippe P Richard, and J Cole Smith. A class of algorithms for mixed-integer bilevel min–max optimization. *Journal of Global Optimization*, 66:225–262, 2016.
- [58] Alan Washburn and Kevin Wood. Two-person zero-sum games for network interdiction. *Operations research*, 43(2):243–251, 1995.
- [59] Noah Weninger and Ricardo Fukasawa. A fast combinatorial algorithm for the bilevel knapsack problem with interdiction constraints. In *International Conference on Integer Programming and Combinatorial Optimization*, pages 438–452. Springer, 2023.
- [60] Manzil Zaheer, Satwik Kottur, Siamak Ravanbakhsh, Barnabas Poczos, Russ R Salakhutdinov, and Alexander J Smola. Deep sets. *Advances in neural information processing systems*, 30, 2017.
- [61] Marco Zugno, Juan Miguel Morales, Pierre Pinson, and Henrik Madsen. A bilevel model for electricity retailers’ participation in a demand response market environment. *Energy Economics*, 36:182–197, 2013.

A Proofs for Section 4.3

Proposition 1. *When applied to a leader decision \mathbf{x}^* returned by the upper-level approximation, the procedure described in Section 4.3 either produces a bilevel-feasible pair $(\mathbf{x}^*, \mathbf{y}^*)$ or declares \mathbf{x}^* as infeasible.*

Proof. If only Assumption 1(b) is satisfied, then Step 1 may detect that the problem $\Phi(\mathbf{x}^*)$ is infeasible, i.e., that there does not exist a $\mathbf{y}' \in \mathcal{Y}$ that satisfies $g(\mathbf{x}^*, \mathbf{y}') \geq \mathbf{0}$ (1c). If Step 1 is feasible, then $\Phi(\mathbf{x}^*)$ is the optimal follower's value for leader decision \mathbf{x}^* . Note that if both Assumptions 1(a) and 1(b) are satisfied, then Step 1 is guaranteed to be feasible. It remains to obtain a corresponding follower solution \mathbf{y}^* that minimizes $F(\mathbf{x}^*, \cdot)$ (1a). Step 2 computes such a \mathbf{y}^* and the bilevel-feasible pair $(\mathbf{x}^*, \mathbf{y}^*)$ is returned. ■

Proposition 2. *When applied to a leader-follower solution pair $(\mathbf{x}^*, \tilde{\mathbf{y}})$ returned by the lower-level approximation, the procedure described in Section 4.3 produces a bilevel-feasible pair $(\mathbf{x}^*, \mathbf{y}^*)$.*

Proof. The lower-level approximation (7) is guaranteed to return a leader decision \mathbf{x}^* for which there exists a follower decision \mathbf{y}^* such that $(\mathbf{x}^*, \mathbf{y}^*)$ is bilevel-feasible. To obtain \mathbf{y}^* , Step 1 first computes the minimum follower value $\Phi(\mathbf{x}^*)$ that must be achieved by any valid follower solution; note that this condition may not have been met by $\tilde{\mathbf{y}}$ as the latter only satisfies $f(\mathbf{x}^*, \tilde{\mathbf{y}}) \geq \text{NN}^l(\mathbf{x}^*; \Theta) - s$ (7d). Step 2 then selects a follower decision which both satisfies $f(\mathbf{x}^*, \mathbf{y}^*) \geq \Phi(\mathbf{x}^*)$ and minimizes $F(\mathbf{x}^*, \cdot)$ (2b). The bilevel-feasible pair $(\mathbf{x}^*, \mathbf{y}^*)$ is returned. ■

B Proofs for Approximation Guarantees of Section 4.6.1

Proof of Lemma 1

Proof. Case 1: Let $\mathbf{x} \in \mathcal{X}$ for which it holds $\text{NN}^l(\mathbf{x}; \Theta) \geq \Phi(\mathbf{x})$ and assume the opposite of the statement is true, i.e., for the optimal reaction $\mathbf{y}_{\text{NN}}^*(\mathbf{x})$ in (7) it holds that $\Phi(\mathbf{x}) > f(\mathbf{x}, \mathbf{y}_{\text{NN}}^*(\mathbf{x}))$. Since $\lambda > 0$ and due to Constraint (7d) the optimal slack value for solution \mathbf{x} in Problem (7) is $s^*(\mathbf{x}, \mathbf{y}) = \text{NN}^l(\mathbf{x}; \Theta) - f(\mathbf{x}, \mathbf{y})$. Assume $\mathbf{y}^*(\mathbf{x})$ is the optimal follower reaction in (2) for \mathbf{x} , then it holds that:

$$\begin{aligned}
 & f(\mathbf{x}, \mathbf{y}_{\text{NN}}^*(\mathbf{x})) + \lambda s^*(\mathbf{x}, \mathbf{y}_{\text{NN}}^*(\mathbf{x})) \\
 &= f(\mathbf{x}, \mathbf{y}_{\text{NN}}^*(\mathbf{x})) + \lambda (\text{NN}^l(\mathbf{x}; \Theta) - f(\mathbf{x}, \mathbf{y}_{\text{NN}}^*(\mathbf{x}))) \\
 &> f(\mathbf{x}, \mathbf{y}_{\text{NN}}^*(\mathbf{x})) + \lambda (\text{NN}^l(\mathbf{x}; \Theta) - f(\mathbf{x}, \mathbf{y}_{\text{NN}}^*(\mathbf{x}))) + (\lambda - 1) (f(\mathbf{x}, \mathbf{y}_{\text{NN}}^*(\mathbf{x})) - f(\mathbf{x}, \mathbf{y}^*(\mathbf{x}))) \\
 &= f(\mathbf{x}, \mathbf{y}^*(\mathbf{x})) + \lambda (\text{NN}^l(\mathbf{x}; \Theta) - f(\mathbf{x}, \mathbf{y}^*(\mathbf{x}))) \\
 &= f(\mathbf{x}, \mathbf{y}^*(\mathbf{x})) + \lambda s^*(\mathbf{x}, \mathbf{y}^*(\mathbf{x}))
 \end{aligned}$$

where the first inequality follows since $\lambda > 1$ and $f(\mathbf{x}, \mathbf{y}^*(\mathbf{x})) = \Phi(\mathbf{x}) > f(\mathbf{x}, \mathbf{y}_{\text{NN}}^*(\mathbf{x}))$ and the latter equality follows from $\text{NN}^l(\mathbf{x}; \Theta) \geq \Phi(\mathbf{x}) = f(\mathbf{x}, \mathbf{y}^*(\mathbf{x}))$. The latter result shows that the solution $(\mathbf{x}, \mathbf{y}^*(\mathbf{x}))$ has a strictly better objective value in the surrogate problem (7) than $(\mathbf{x}, \mathbf{y}_{\text{NN}}^*(\mathbf{x}))$ which contradicts the optimality of $(\mathbf{x}, \mathbf{y}_{\text{NN}}^*(\mathbf{x}))$.

Case 2: Let $\mathbf{x} \in \mathcal{X}$ be a leader's decision for which $\text{NN}^l(\mathbf{x}; \Theta) < \Phi(\mathbf{x})$ and assume the opposite of the statement, i.e., for the optimal reaction $\mathbf{y}_{\text{NN}}^*(\mathbf{x})$ in (7) it holds that $\text{NN}^l(\mathbf{x}; \Theta) - \frac{1}{\lambda}\Delta > f(\mathbf{x}, \mathbf{y}_{\text{NN}}^*(\mathbf{x}))$. Hence the optimal slack value in (7) is

$$s^*(\mathbf{x}, \mathbf{y}_{\text{NN}}^*(\mathbf{x})) = \text{NN}^l(\mathbf{x}; \Theta) - f(\mathbf{x}, \mathbf{y}_{\text{NN}}^*(\mathbf{x})) > \frac{1}{\lambda}\Delta. \quad (9)$$

First, assume there exists another feasible solution $\bar{\mathbf{y}}(\mathbf{x})$ for Problem (7) with

$$f(\mathbf{x}, \mathbf{y}_{\text{NN}}^*(\mathbf{x})) < f(\mathbf{x}, \bar{\mathbf{y}}(\mathbf{x})) < \text{NN}^l(\mathbf{x}; \Theta)$$

then solution $(\mathbf{x}, \bar{\mathbf{y}}(\mathbf{x}))$ has a strictly better objective value than $(\mathbf{x}, \mathbf{y}_{\text{NN}}^*(\mathbf{x}))$ in (7) since increasing the value of f by δ decreases the value of the slack variable by δ which results in a better objective value since $\lambda > 1$, which contradicts the optimality of $(\mathbf{x}, \mathbf{y}_{\text{NN}}^*(\mathbf{x}))$.

Second, assume there exists no other feasible solution $\bar{\mathbf{y}}(\mathbf{x})$ for Problem (7) with

$$f(\mathbf{x}, \mathbf{y}_{\text{NN}}^*(\mathbf{x})) < f(\mathbf{x}, \bar{\mathbf{y}}(\mathbf{x})) < \text{NN}^l(\mathbf{x}; \Theta).$$

Then there must exist a feasible solution $\bar{\mathbf{y}}(\mathbf{x})$ with $f(\mathbf{x}, \bar{\mathbf{y}}(\mathbf{x})) \geq \text{NN}^l(\mathbf{x}; \Theta)$ and

$$f(\mathbf{x}, \bar{\mathbf{y}}(\mathbf{x})) - f(\mathbf{x}, \mathbf{y}_{\text{NN}}^*(\mathbf{x})) \leq \Delta, \quad (10)$$

by definition of Δ . In this case, we have

$$\begin{aligned} & f(\mathbf{x}, \mathbf{y}_{\text{NN}}^*(\mathbf{x})) + \lambda s^*(\mathbf{x}, \mathbf{y}_{\text{NN}}^*(\mathbf{x})) - f(\mathbf{x}, \bar{\mathbf{y}}(\mathbf{x})) - \lambda s^*(\mathbf{x}, \bar{\mathbf{y}}(\mathbf{x})) \\ &= f(\mathbf{x}, \mathbf{y}_{\text{NN}}^*(\mathbf{x})) + \lambda s^*(\mathbf{x}, \mathbf{y}_{\text{NN}}^*(\mathbf{x})) - f(\mathbf{x}, \bar{\mathbf{y}}(\mathbf{x})) \\ &> f(\mathbf{x}, \mathbf{y}_{\text{NN}}^*(\mathbf{x})) + \Delta - f(\mathbf{x}, \bar{\mathbf{y}}(\mathbf{x})) \geq -\Delta + \Delta = 0, \end{aligned}$$

where the first equality follows since $s^*(\mathbf{x}, \bar{\mathbf{y}}(\mathbf{x})) = 0$, the first inequality follows from (9) and the last inequality follows from (10). In summary, the latter results show that there exists a solution $(\mathbf{x}, \bar{\mathbf{y}}(\mathbf{x}))$ for (7) which has strictly better objective value than $(\mathbf{x}, \mathbf{y}_{\text{NN}}^*(\mathbf{x}))$ which is a contradiction.

Note that the inequality $f(\mathbf{x}, \mathbf{y}_{\text{NN}}^*(\mathbf{x})) \leq \Phi(\mathbf{x})$ follows directly from the definition of $\Phi(\mathbf{x})$. ■

Proof of Theorem 1

Proof. Let $(\mathbf{x}_{\text{NN}}^*, \mathbf{y}_{\text{NN}}^*)$ be an optimal solution of the surrogate problem (7). By Lemma 1 and by definition (8) it follows that

$$\begin{aligned} \Phi(\mathbf{x}_{\text{NN}}^*) &\geq f(\mathbf{x}_{\text{NN}}^*, \mathbf{y}_{\text{NN}}^*) \geq \text{NN}^l(\mathbf{x}_{\text{NN}}^*; \Theta) - \frac{1}{\lambda}\Delta \\ &\geq \Phi(\mathbf{x}_{\text{NN}}^*) - \alpha - \frac{1}{\lambda}\Delta. \end{aligned} \quad (11)$$

Following the three steps presented in Section 4.3, NEUR2BiLO returns a feasible solution $(\mathbf{x}^*, \mathbf{y}^*)$ for Problem (2) where $\mathbf{x}^* = \mathbf{x}_{\text{NN}}^*$ and $f(\mathbf{x}^*, \mathbf{y}^*) = \Phi(\mathbf{x}^*)$. Hence the following holds:

$$f(\mathbf{x}^*, \mathbf{y}^*) = \Phi(\mathbf{x}^*) \leq f(\mathbf{x}^*, \mathbf{y}_{\text{NN}}^*) + \alpha + \frac{1}{\lambda}\Delta. \quad (12)$$

Assume $(\mathbf{x}^{**}, \mathbf{y}^{**})$ is an optimal bilevel solution of Problem (1) and $\mathbf{y}_{\text{NN}}^{**}$ the optimal follower response in the surrogate problem (7). Then we have

$$f(\mathbf{x}^*, \mathbf{y}_{\text{NN}}^*) + \mathbf{s}^*(\mathbf{x}^*, \mathbf{y}_{\text{NN}}^*) \leq f(\mathbf{x}^{**}, \mathbf{y}_{\text{NN}}^{**}) + \mathbf{s}^*(\mathbf{x}^{**}, \mathbf{y}_{\text{NN}}^{**})$$

since $(\mathbf{x}_{\text{NN}}^*, \mathbf{y}_{\text{NN}}^*)$ is an optimal solution of (7) with objective value given by (7a). From the latter inequality we obtain

$$\begin{aligned} f(\mathbf{x}^*, \mathbf{y}_{\text{NN}}^*) &\leq f(\mathbf{x}^{**}, \mathbf{y}_{\text{NN}}^{**}) + \mathbf{s}^*(\mathbf{x}^{**}, \mathbf{y}_{\text{NN}}^{**}) - \mathbf{s}^*(\mathbf{x}^*, \mathbf{y}_{\text{NN}}^*) \\ &\leq f(\mathbf{x}^{**}, \mathbf{y}^{**}) + \mathbf{s}^*(\mathbf{x}^{**}, \mathbf{y}_{\text{NN}}^{**}) \\ &\leq f(\mathbf{x}^{**}, \mathbf{y}^{**}) + \text{NN}^l(\mathbf{x}^{**}; \Theta) - f(\mathbf{x}^{**}, \mathbf{y}_{\text{NN}}^{**}) \\ &\leq f(\mathbf{x}^{**}, \mathbf{y}^{**}) + \Phi(\mathbf{x}^{**}) + \alpha - (\Phi(\mathbf{x}^{**}) - \alpha - \frac{1}{\lambda}\Delta) \\ &= \text{opt} + 2\alpha + \frac{1}{\lambda}\Delta \end{aligned}$$

where the second inequality follows from $\mathbf{s}^*(\mathbf{x}^*, \mathbf{y}_{\text{NN}}^*) \geq 0$ and \mathbf{y}^{**} being an optimal follower solution for \mathbf{x}^{**} . The third inequality follows from Observation 1 and the fourth inequality follows from (8) and from (11) applied to \mathbf{x}^{**} .

Together with (12), this completes the proof. ■

C Problem Formulations

C.1 Knapsack interdiction

The bilevel knapsack problem with interdiction constraints as described in Tang et al. [57] is given by

$$\begin{aligned} \min_{\mathbf{x} \in \{0,1\}^n, \mathbf{y}} \quad & \sum_{i=1}^n p_i y_i \\ \text{s.t.} \quad & \sum_{i=1}^n x_i \leq k, \\ & \mathbf{y} \in \arg \max_{\mathbf{y}' \in \{0,1\}^n} \sum_{i=1}^n p_i y'_i \\ & \text{s.t.} \quad \sum_{i=1}^n a_i y'_i \leq b, \\ & \quad y'_i + x_i \leq 1, i \in [n], \end{aligned}$$

where \mathbf{x} are the leader's variables and \mathbf{y} are that of the follower. The leader decides to interdict (a maximum of k) items of the knapsack solved in the follower's problem with n the number of items, p_i the profits, a_i the weight of item i , respectively, and the budget of

the knapsack is denoted by b . The original instances from Tang et al. [57] are available here² and all evaluation instances in the MibS input file format³ are available here⁴.

C.2 Critical node problem

The critical node problem is described in Carvalho et al. [13] as follows

$$\begin{aligned}
& \max_{\mathbf{x} \in \{0,1\}^n, \mathbf{y}} && \sum_{i=1}^n \left(p_i^d \left((1-x_i)(1-y_i) + \eta x_i y_i + \epsilon x_i (1-y_i) + \delta (1-x_i) y_i \right) \right) \\
& \text{s.t.} && \sum_{i=1}^n d_i x_i \leq D, \\
& && \mathbf{y} \in \arg \max_{\mathbf{y}' \in \{0,1\}^n} \sum_{i=1}^n \left(p_i^a \left(-\gamma (1-x_i)(1-y'_i) + (1-x_i)y'_i + (1-\eta)x_i y'_i \right) \right) \\
& && \text{s.t.} \quad \sum_{i=1}^n a_i y'_i \leq A,
\end{aligned}$$

where \mathbf{x} and \mathbf{y} are the leader's and follower's variables, respectively. Here, \mathbf{x} denotes the decisions of the leader (defender) who selects which nodes to deploy resources to defend a set of nodes, while \mathbf{y} are the decisions for the follower (attacker) for which nodes to attack. d_i and a_i are the costs for the x_i and y_i , respectively. D and A are the budgets for the defender and attacker, respectively. In this problem, the bilinearity arises in the objectives of both the leader and follower, which results in 4 outcomes for each possible combination of defending and attacking a node i . The first outcome arises when both the leader and follower do not select the node. In this case, the leader receives the full profit, p_i^d , and the follower pays an opportunity cost of $-\gamma p_i^a$ for not attacking an undefended node. Second is a success attack, wherein the leader receives a reduced profit of δp_i^d and the follower receives the full profit p_i^a . Third is a mitigated attack, wherein the leader receives a profit of ηp_i^d for a degradation in operations, while the follower receives a profit of $(1-\eta)p_i^a$ for a mitigated attack. Fourth is a mitigation without an attack, wherein the leader receives a profit of ϵp_i^d for a degradation in operations, while the follower receives a profit of 0 for a mitigated attack. Our evaluation instances in the MibS input file format are available here⁵.

²https://github.com/khalil-research/Neur2BiLO/tree/main/data/kp/BKPIns_ver2

³<https://coral.ise.lehigh.edu/data-sets/bilevel-instances/>

⁴https://github.com/khalil-research/Neur2BiLO/tree/main/data/kp/solver_instances

⁵https://github.com/khalil-research/Neur2BiLO/tree/main/data/cng/solver_instances

C.3 Donor-recipient problem

The donor-recipient problem as described in Ghatkar et al. [29], and introduced in Morton et al. [46], is formulated as

$$\begin{aligned}
 & \max_{\mathbf{x} \in [0,1]^n, \mathbf{y}, y_0} \sum_{i=1}^n w_i y_i \\
 & \text{s.t.} \quad \sum_{i=1}^n c_i x_i \leq B_d, \\
 & (\mathbf{y}, y_0) \in \arg \max_{\mathbf{y}' \in \{0,1\}^n, y'_0 \in [0,1]} \sum_{i=1}^n v_i y'_i + v_0 y'_0 \\
 & \text{s.t.} \quad \sum_{i=1}^n (c_i - c_i x_i) y'_i + c_0 y'_0 \leq B_r,
 \end{aligned}$$

where the leader’s decisions \mathbf{x} represent those of the donor and the follower decisions (\mathbf{y}, y_0) the ones of the recipient. The profit of project i is given as w_i for the leader and v_i for the follower, the cost as c_i , and the budget of the leader, resp. follower, as B_d and B_r . Next to the projects, the recipient can allocate its budget to external projects, for which the profit is given as v_0 and the cost c_0 . The evaluation instances dataset 15 for DRP are available from the author⁶.

C.4 Discrete network design problem

We use the standard formulation from Section 1 following the computational benchmarking study of Rey [50] and the code provided by the author⁷.

D Machine Learning Details

D.1 Models, Features, & Hyperparameters

For all problems, we derive features that correspond to each upper-level decision variable, as well as general instance features.

D.1.1 KIP, CNP, DRP

For KIP, CNP, DRP, we have both n decisions in the upper- and lower-level of the problems. For the learning model, we utilize a set-based architecture [60], wherein we first represent the objective and constraint coefficients for each upper-level and lower-level decision, independent of the decision (\mathbf{f}_i). Each of these are passed through a feed-forward network with shared parameters (Ψ_d) to compute an m -dimension embedding. The embeddings

⁶<https://github.com/ashwin-1983/DR-BKP/>

⁷<https://github.com/davidrey123/DNDP/>

are then summed and passed through another feed-forward network (Ψ_s) to compute the instance’s k -dimensional embedding. This instance embedding is then concatenated with features related to the upper- and lower-level that are dependent on the decision ($h(\mathbf{x}_i)$). The concatenated vector is passed through a feed-forward network with shared parameters (Ψ_v) to predict n scalar values (i.e., one for each decision). The final prediction is equal to the dot product of the n predictions with the objective function coefficients of the upper- or lower-level problem, depending on the type of value function approximation. This final step exploits the separable nature of the objective functions in question as they can all be expressed as $\sum_{i=1}^n c_i z_i$, where c_i is a *known* coefficient and z_i is a decision variable or a function of a set of decision variables with index i . The objectives for KIP, CNP, and DRP all satisfy this property. We leverage this knowledge of the coefficients of separable objective functions as an inductive bias in the design of the learning architecture to facilitate convergence to accurate models. The decision-dependent and decision-independent features are summarized in Table 6.

One minor remark for KIP is that since it is an interdiction problem, we multiply the concatenated vector, i.e., the input to Φ_v , by $(1 - x_i)$ as a mask given that the follower cannot select the same items as the leader.

For all instances, we do not perform systematic hyperparameter tuning. The sub-networks Ψ_d , Ψ_s , Ψ_v are feed-forward networks with 1 hidden layer of dimension 128. The decision-independent feature embedding dimension (m) is 64, and the instance embedding dimension (k) is 32. We use a batch size of 32, a learning rate of 0.01, and Adam [33] as an optimizer.

Problem	Type	Features
KIP	\mathbf{f}_i $h(\mathbf{x}_i)$	$\frac{p_i/a_i}{\max_i\{p_i/a_i\}}, p_i, a_i, k/n, x_i^{dg}, y_i^{dg}, obj^{dg}/n$ \mathbf{f}_i, x_i, y_i^g
CNP	\mathbf{f}_i $h(\mathbf{x}_i)$	$\frac{p_i^d/d_i}{\max_i\{p_i^d/d_i\}}, \frac{p_i^a/a_i}{\max_i\{p_i^a/a_i\}}, d_i, a_i, p_i^a, p_i^d, \gamma, \eta, \epsilon, \delta, A, D$ $\mathbf{f}_i, x_i, -\gamma(1 - x_i), (1 - x_i), (1 - \eta)x_i$
DRP	\mathbf{f}_i $h(\mathbf{x}_i)$	$\frac{w_i/c_i}{\max_i\{w_i/c_i\}}, \frac{v_i/c_i}{\max_i\{c_i/v_i\}}, w_i, v_i, c_i, B_d, B_r$ \mathbf{f}_i, x_i

Table 6: Features for KIP, CNP, and DRP. Most features are derived directly from the objective and constraint coefficients, so refer to Appendix C for the definitions. For KIP, additional features are computed using simple greedy heuristics. For the KIP DIF, we compute $x_i^{dg}, y_i^{dg}, obj^{dg}$, which correspond to a purely greedy strategy, i.e., the upper-level interdicts the k items with the largest profit to cost ratio (p_i/a_i) and the lower-level decisions are the largest remaining highest profit to cost ratio items. For $h(\mathbf{x}_i)$ in KIP, we also include lower-level decisions based on G-VFA (y_i^g).

D.1.2 DNDP

We train neural network models (one hidden layer, 16 neurons, a learning rate of 0.01 with the Adam optimizer) and gradient-boosted trees (default scikit-learn hyperparameters, except for `n_estimators = 50`). The inputs to these models are 30-dimensional binary vectors representing the subset of links selected by the leader.

D.2 Data Collection & Training Times

For KIP, CNP, DRP, we sample 1,000 instances according to the procedures specified in Tang et al. [57], Dragotto et al. [20], and Ghatkar et al. [29], respectively. For each instance, we sample 100 upper-level decisions, i.e., 100,000 samples in total. Additionally, for KIP, CNP, DRP, the lower-level problems are solved with 30 CPUs in parallel. For training, we train for 1,000 epochs. However, if the validation mean absolute error does not improve in 200 iterations, we terminate early. Data collection and training times are reported in Table 7.

For DNDP, we use the Sioux Falls transportation network provided by [50] along with the author’s 60 test instances. All instances use the same base network with different sets of candidate links to add and different budgets. There are 30 candidate links in total, and each test instance involves a subset of 10 or 20 of these links. To construct a training set, we sample 1000 leader decisions by first uniformly sampling an integer between 1 and 20, then uniformly sampling that many candidate links out of the set of 30 options; samples with total cost exceeding 50% of the total cost of all 30 edges are rejected as they are likely to exceed realistic budgets.

E Ablation Studies

E.1 Lower-Level Value Function Constraints

In this section, we present an ablation study comparing alternative types of value function approximation (VFA) for the lower-level approximation on the KIP. Namely, we compare the approach used in the main paper, NN^l , which utilizes a slack variable to ensure feasibility. In addition, we include NN^n which does not use a slack at all, and NN^d , which uses the largest error in the validation set to scale the prediction down. Table 8 reports objectives, relative errors, and solving times of each method. In general, the solution quality of NN^l slightly exceeds that of NN^d , while NN^n does significantly worse. The latter results is unsurprising given that any underestimation will cause a loss of feasibility for potentially high quality upper-level decisions. NN^l is additionally generally the fastest to optimize as well.

E.2 The effect of λ

In this section, we present a brief set of results for the use of $\lambda = 0.1$ for DNDP. Table 9 presents relative error and solving times for this setting. Notably, this choice of λ tends to

Instance	Data Collection	Training Time	
		Lower	Upper
KIP ($n = 18$)	142.08	2576.43	-
KIP ($n = 20$)	172.65	4714.88	-
KIP ($n = 22$)	141.61	2346.20	-
KIP ($n = 25$)	170.30	4007.75	-
KIP ($n = 28$)	142.34	2684.80	-
KIP ($n = 30$)	168.91	1835.27	-
KIP ($n = 100$)	164.16	3467.26	-
CNP ($ V = 10$)	1,397.58	1839.60	4670.87
CNP ($ V = 25$)	1,522.32	2072.60	4841.31
CNP ($ V = 50$)	1,823.16	2103.50	2963.64
CNP ($ V = 100$)	1,872.07	1944.08	2931.43
CNP ($ V = 300$)	3,662.89	3800.02	3598.04
CNP ($ V = 500$)	4,742.06	2263.68	6214.35
DRP	1939.24	1768.82	1784.15
DNDP	~ 300.0	~ 5.0	~ 5.0

Table 7: Data collection and training times for all problems. Note that as KIP is an interdiction problem, the same trained model can be used for the upper- and lower-level approximation, so we simply leave the upper-level as - for this problem. All times in seconds.

n	k	Objective			Mean Relative Error (%)			Times		
		NN^l	NN^d	NN^n	NN^l	NN^d	NN^n	NN^l	NN^d	NN^n
18	5	308.30	308.40	318.40	0.00	0.03	3.28	0.59	0.83	1.06
18	9	145.60	145.60	152.90	0.00	0.00	6.70	0.59	1.21	0.81
18	14	31.00	37.50	40.00	0.00	16.91	48.23	0.22	0.32	0.35
20	5	390.30	390.30	413.90	0.00	0.00	6.48	0.62	0.79	1.38
20	10	165.40	165.40	175.90	0.00	0.00	6.60	0.66	1.47	1.76
20	15	33.40	32.50	55.70	3.33	14.29	100.91	0.32	0.38	0.96
22	6	385.50	386.80	403.00	0.00	0.27	4.56	0.19	0.37	0.80
22	11	163.20	162.10	179.20	0.55	0.07	11.83	0.28	0.85	1.23
22	17	35.20	35.20	49.00	5.15	4.63	69.91	0.24	0.19	0.41
25	7	438.20	438.20	446.50	0.00	0.00	1.98	2.66	2.40	3.85
25	13	194.90	195.50	206.50	0.00	0.26	6.67	2.75	3.25	4.83
25	19	43.30	43.30	64.40	1.69	1.69	92.49	0.48	0.74	1.84
28	7	518.30	518.30	532.20	0.00	0.00	2.80	0.67	0.83	2.37
28	14	224.90	224.90	234.70	0.00	0.00	4.60	2.10	2.69	3.72
28	21	46.70	49.90	60.70	0.00	7.48	37.45	0.45	0.83	1.67
30	8	536.30	537.10	537.70	0.00	0.18	0.25	1.54	1.86	3.07
30	15	231.20	231.20	232.80	0.16	0.16	0.82	3.64	4.18	5.03
30	23	49.00	50.70	51.90	0.00	2.79	4.48	1.08	1.50	1.76
100	25	2,164.71	2,164.13	2,168.52	0.04	0.01	0.22	10.02	12.28	19.81
100	50	965.37	965.26	974.28	0.03	0.02	1.01	51.68	61.09	72.86
100	75	245.01	245.10	262.66	0.04	0.08	8.18	24.69	30.48	81.30

Table 8: KIP results comparing NN^l , NN^d , and NN^n . Each row averaged over 10 instances, except for $n = 100$, which is average over 100 instances. All times in seconds.

provide higher quality solutions to $\lambda = 1$, as reported in the main paper in Table 5, which motivates a clear direction for easy improvement of the already strong numerical results reported for DNDP, as well as for the other problems.

# of edges	budget	NN ^l		NN ^u		GBT ^l		GBT ^u		MKKT		
		MRE	Time	MRE	Time	MRE	Time	MRE	Time	MRE-5	MRE-10	MRE-30
10	25%	0.15	2.66	4.97	0.01	0.16	3.38	1.11	0.04	6.08	0.51	0.10
10	50%	0.03	2.43	3.93	0.01	0.03	3.46	3.70	0.05	7.39	2.17	0.00
10	75%	0.02	1.61	1.49	0.01	0.01	1.67	1.99	0.03	5.87	0.05	0.06
20	25%	1.85	5.01	7.42	0.04	1.48	5.00	4.70	0.26	12.98	6.44	0.86
20	50%	1.20	5.01	4.40	0.05	0.30	5.01	2.75	0.15	16.50	9.11	0.94
20	75%	0.07	2.23	4.87	0.01	0.07	2.79	0.84	0.10	11.02	4.07	0.08
Average		0.55	3.16	4.51	0.02	0.34	3.55	2.51	0.11	9.97	3.72	0.34

Table 9: DNDP results for $\lambda = 0.1$. Each is averaged across 10 instances. NN^l and GBT^l are the learning-based formulations with slack for the lower-level approximation. NN^u and GBT^u are the learning-based formulations for the upper-level approximation.

E.3 Greedy Features for Knapsack

This section explores the impact of the use of greedy features on the KIP problem. We specifically compare a model trained purely on the coefficients to a model trained on the coefficients with additional features derived from KIP-specific greedy heuristics. From Table 10, there is a clear advantage with the greedy features in terms of solution quality at the cost of increased solving time.

F Objective & Incumbent Results

This section reports the more detailed information related to the objective values for each problem. Objective results for each problem are given in Tables 11-14. In addition, for KIP and CNP, as the solver from Fischetti et al. [25] provides easily accessible incumbent solutions, we include two additional metrics.

- The first metric “Solver Time Ratio” measures the time it takes the solver to obtain an equally good (or better) incumbent solution, divided by the solving time of the respective approximation. The number in brackets to the right indicates the number of instances for which the solver finds an equivalent solution.
- The second metric “Solver Relative Error at Time” measures the relative error of the best solution found by the solver compared to the respective approximation. The value in brackets to the right indicates the number of instances for which the solver finds an incumbent before the approximation is done solving.

n	k	Objective		Mean Relative Error (%)		Times	
		NN ^l greedy	NN ^l no greedy	NN ^l greedy	NN ^l no greedy	NN ^l greedy	NN ^l no greedy
18	5	308.30	314.90	0.85	2.93	0.59	0.06
18	9	145.60	150.50	1.17	4.28	0.59	0.07
18	14	31.00	41.60	0.00	55.04	0.22	0.05
20	5	390.30	404.40	0.00	3.71	0.62	0.06
20	10	165.40	172.00	0.55	4.06	0.66	0.05
20	15	33.40	36.50	0.00	7.31	0.32	0.06
22	6	385.50	390.60	0.59	1.88	0.19	0.07
22	11	163.20	170.80	0.00	4.31	0.28	0.07
22	17	35.20	39.10	7.91	31.93	0.24	0.06
25	7	438.20	446.30	0.11	1.67	2.66	0.08
25	13	194.90	197.20	0.89	2.58	2.75	0.07
25	19	43.30	49.10	0.00	13.53	0.48	0.07
28	7	518.30	537.70	0.15	3.63	0.67	0.07
28	14	224.90	225.90	0.21	0.61	2.10	0.08
28	21	46.70	52.10	0.00	11.85	0.45	0.08
30	8	536.30	556.50	0.00	3.61	1.54	0.08
30	15	231.20	233.70	0.21	1.20	3.64	0.09
30	23	49.00	51.30	0.00	4.97	1.08	0.08
100	25	2,164.71	2,473.08	0.00	14.22	10.02	0.54
100	50	965.37	1,062.92	0.04	10.23	51.68	0.52
100	75	245.01	313.44	0.00	27.62	24.69	0.53

Table 10: KIP results comparing NN^l with and without greedy-based features NN^d. Each row averaged over 10 instances, except for $n = 100$, which is an average over 100 instances. All times in seconds.

n	k	Objective				Mean Relative Error (%)				Solving Time				Solver Time Ratio			Solver Relative Error at Time		
		NN ^l	NN ^u	G-VFA	B&C	NN ^l	NN ^u	G-VFA	B&C	NN ^l	NN ^u	G-VFA	B&C	NN ^l	NN ^u	G-VFA	NN ^l	NN ^u	G-VFA
18	5	308.30	308.30	309.20	303.50	1.48	1.48	1.82	0.00	0.59	0.34	0.14	9.55	24.48 (10)	35.86 (10)	177.39 (10)	- (0)	- (0)	- (0)
18	9	145.60	145.60	149.10	143.40	1.51	1.51	3.97	0.00	0.59	0.43	0.22	5.81	12.31 (10)	18.52 (10)	73.49 (10)	- (0)	- (0)	- (0)
18	14	31.00	31.00	51.40	31.00	0.00	0.00	64.22	0.00	0.22	0.17	0.03	0.39	1.87 (10)	2.86 (10)	31.9 (10)	44.0 (2)	41.5 (2)	- (0)
20	5	390.30	390.30	397.60	388.50	0.41	0.41	2.19	0.00	0.62	0.45	0.25	23.18	50.68 (10)	65.56 (10)	420.04 (10)	- (0)	- (0)	- (0)
20	10	165.40	165.40	165.40	163.70	0.99	0.99	0.99	0.00	0.66	0.58	0.36	10.27	18.39 (10)	22.03 (10)	80.0 (10)	- (0)	- (0)	- (0)
20	15	33.40	33.40	41.90	31.40	3.57	3.57	23.39	0.00	0.32	0.19	0.02	0.94	2.82 (10)	4.75 (10)	54.29 (10)	- (0)	- (0)	- (0)
22	6	385.50	385.50	384.30	382.70	0.71	0.71	0.42	0.00	0.19	0.18	0.18	42.30	228.97 (10)	249.8 (10)	714.31 (10)	- (0)	- (0)	- (0)
22	11	163.20	163.20	163.30	161.00	1.01	1.01	1.08	0.00	0.28	0.28	0.33	16.26	69.05 (10)	74.99 (10)	129.04 (10)	- (0)	- (0)	- (0)
22	17	35.20	35.20	35.20	29.20	14.43	14.43	14.43	0.00	0.24	0.15	0.13	0.68	3.09 (10)	5.48 (10)	29.34 (10)	18.0 (1)	- (0)	- (0)
25	7	438.20	438.20	438.20	436.20	0.44	0.44	0.44	0.00	2.66	2.42	0.64	137.96	58.27 (10)	61.24 (10)	1102.38 (10)	28.69 (2)	28.69 (2)	28.69 (2)
25	13	194.90	194.90	199.90	191.50	1.42	1.42	3.85	0.00	2.75	2.79	1.24	48.43	21.14 (10)	25.13 (10)	67.86 (10)	- (0)	- (0)	- (0)
25	19	43.30	43.30	43.30	41.80	2.49	2.49	2.49	0.00	0.48	0.38	0.13	1.77	3.98 (10)	4.81 (10)	38.29 (10)	- (0)	- (0)	- (0)
28	7	518.30	518.30	517.60	516.10	0.39	0.39	0.26	0.00	0.67	0.74	0.62	309.18	671.57 (10)	518.35 (10)	1033.45 (10)	29.28 (8)	29.28 (8)	29.48 (8)
28	14	224.90	224.90	226.80	223.40	0.75	0.75	1.37	0.00	2.10	1.45	1.29	120.74	59.99 (10)	84.36 (10)	120.05 (10)	19.84 (2)	19.84 (2)	16.14 (2)
28	21	46.70	46.70	48.20	46.20	1.14	1.14	3.16	0.00	0.45	0.49	0.31	4.92	12.95 (10)	11.66 (10)	38.98 (10)	- (0)	- (0)	- (0)
30	8	536.30	536.30	538.70	536.30	0.00	0.00	0.43	0.00	1.54	1.54	0.97	792.44	497.06 (10)	455.29 (10)	1924.47 (10)	27.07 (10)	27.07 (10)	26.58 (10)
30	15	231.20	231.20	231.90	230.00	0.49	0.49	0.75	0.00	3.64	3.06	1.35	187.23	56.14 (10)	66.07 (10)	254.88 (10)	86.11 (6)	86.11 (6)	85.19 (6)
30	23	49.00	49.00	50.40	47.50	2.29	2.29	4.48	0.00	1.08	0.73	0.25	5.65	7.5 (10)	8.79 (10)	48.27 (10)	- (0)	- (0)	- (0)
100	25	2,164.71	2,164.69	2,145.07	2,318.99	0.93	0.93	0.00	8.09	10.02	8.40	4.19	3,600.40	- (0)	- (0)	- (0)	34.36 (100)	34.99 (100)	37.93 (100)
100	50	965.37	965.37	956.76	1,043.71	0.96	0.96	0.04	8.96	51.68	49.28	53.74	3,600.44	23.56 (5)	26.24 (5)	- (0)	59.36 (100)	60.81 (100)	60.48 (100)
100	75	245.01	245.01	245.08	259.95	0.08	0.08	0.12	5.87	24.69	23.78	35.27	3,600.52	133.35 (4)	152.72 (4)	138.07 (5)	177.01 (100)	196.86 (100)	193.94 (100)

Table 11: KIP objective and incumbent results. Each row averaged over 10 instances, except for $n = 100$, which is average over 100 instances. NN^l and NN^u specify the lower- and upper-level approximations respectively. All times in seconds.

V	Objective			Mean Relative Error (%)			Times			Solver Time Ratio		Solver Relative Error at Time	
	NN ^l	NN ^u	B&C	NN ^l	NN ^u	B&C	NN ^l	NN ^u	B&C	NN ^l	NN ^u	NN ^l	NN ^u
10	224.47	225.10	228.63	3.20	2.75	1.01	1.69	1.19	3,600.80	136.66 (288)	191.34 (289)	269.0 (1)	- (0)
25	562.72	566.23	572.51	2.60	1.77	0.73	1.69	1.19	3,600.80	736.84 (275)	3934.02 (271)	2.22 (248)	2.57 (124)
50	1,139.27	1,143.95	1,148.17	1.42	0.98	0.67	1.69	1.19	3,600.80	718.74 (225)	3840.41 (183)	1.94 (295)	3.17 (190)
100	2,285.15	2,297.47	2,272.30	1.12	0.56	1.79	1.69	1.19	3,600.80	645.37 (131)	926.6 (90)	2.4 (283)	2.96 (278)
300	6,781.91	6,882.42	6,755.07	2.01	0.33	2.32	1.69	1.19	3,600.80	41.65 (166)	167.38 (47)	1.49 (245)	2.65 (243)
500	11,348.60	11,439.25	11,208.43	1.33	0.45	2.47	1.69	1.19	3,600.80	106.9 (83)	99.48 (15)	1.51 (206)	2.45 (205)

Table 12: CNP objective and incumbent results. Each row averaged over 300 instances. All times in seconds.

Instance #	Objective			Relative Error (%)			Times		
	NN ^l	NN ^u	B&C+	NN ^l	NN ^u	B&C+	NN ^l	NN ^u	B&C+
1	34,356.00	59,524.00	47,206.00	42.28	0.00	20.69	0.09	1.44	3,600.09
2	33,713.00	54,764.00	39,526.00	38.44	0.00	27.82	0.12	1.52	3,600.08
3	36,717.00	66,967.00	46,792.00	45.17	0.00	30.13	0.14	2.85	3,600.07
4	36,414.00	54,908.00	44,486.00	33.68	0.00	18.98	0.07	1.68	3,637.23
5	33,090.00	59,627.00	43,355.00	44.51	0.00	27.29	0.10	1.96	3,600.07
6	36,691.00	56,603.00	39,006.00	35.18	0.00	31.09	0.08	2.93	3,600.10
7	31,354.00	55,569.00	43,443.00	43.58	0.00	21.82	0.09	1.58	3,600.14
8	35,710.00	54,414.00	39,839.00	34.37	0.00	26.79	0.09	0.87	3,600.10
9	38,961.00	61,869.00	45,288.00	37.03	0.00	26.80	0.16	4.55	3,600.16
10	36,965.00	60,488.00	43,194.00	38.89	0.00	28.59	0.12	3.57	3,600.10
Averaged	35,397.10	58,473.30	43,213.50	39.31	0.00	26.00	0.11	2.30	3,603.82

Table 13: DRP objective results. Each row corresponds to a single instance from dataset 15, i.e., the most challenging instances from Ghatkar et al. [29]. All times in seconds.

# of edges	budget	Objective						Relative Error (%)						Times					
		NN ^l	NN ^u	GBT ^l	GBT ^u	MKKT-5	MKKT-10	MKKT-30	NN ^l	NN ^u	GBT ^l	GBT ^u	MKKT-5	MKKT-10	MKKT-30	NN ^l	NN ^u	GBT ^l	GBT ^u
10	25%	6,181.42	6,422.90	6,206.74	6,194.40	6,502.62	6,155.69	6,129.65	0.88	4.97	1.21	1.11	6.08	0.51	0.10	2.89	0.01	4.02	0.04
10	50%	5,495.55	5,706.80	5,497.17	5,691.26	5,901.07	5,618.41	5,492.23	0.06	3.93	0.09	3.70	7.39	2.17	0.00	3.20	0.01	3.68	0.05
10	75%	5,185.31	5,254.89	5,191.29	5,279.07	5,481.49	5,180.90	5,181.30	0.13	1.49	0.24	2.00	5.88	0.05	0.06	2.15	0.01	2.21	0.03
20	25%	5,207.84	5,554.08	5,263.34	5,415.21	5,842.68	5,539.32	5,215.02	1.16	7.91	2.17	5.21	13.52	6.84	1.33	5.01	0.04	5.01	0.26
20	50%	4,371.18	4,491.25	4,352.48	4,418.78	5,006.37	4,752.99	4,342.83	1.45	4.30	1.02	2.65	16.39	9.02	0.84	5.01	0.05	5.00	0.15
20	75%	4,049.98	4,239.73	4,047.25	4,078.57	4,484.67	4,226.19	4,047.56	0.14	4.87	0.08	0.84	11.02	4.07	0.08	2.48	0.01	3.53	0.10

Table 14: DNDP objective results. Each is averaged across 10 instances. All times in seconds.

G Distributional Results for Relative Error

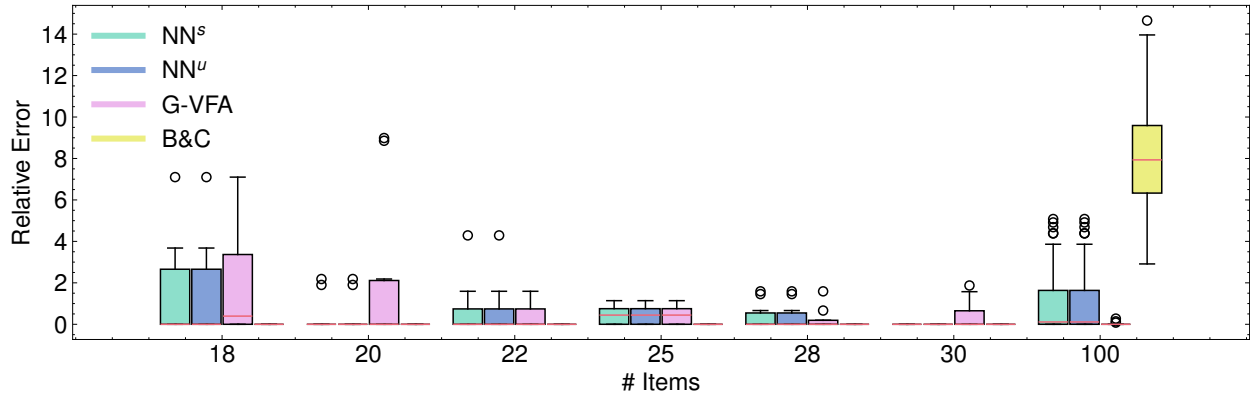


Figure 1: Box plot of relative errors for KIP with interdiction budget of $k = n/4$.

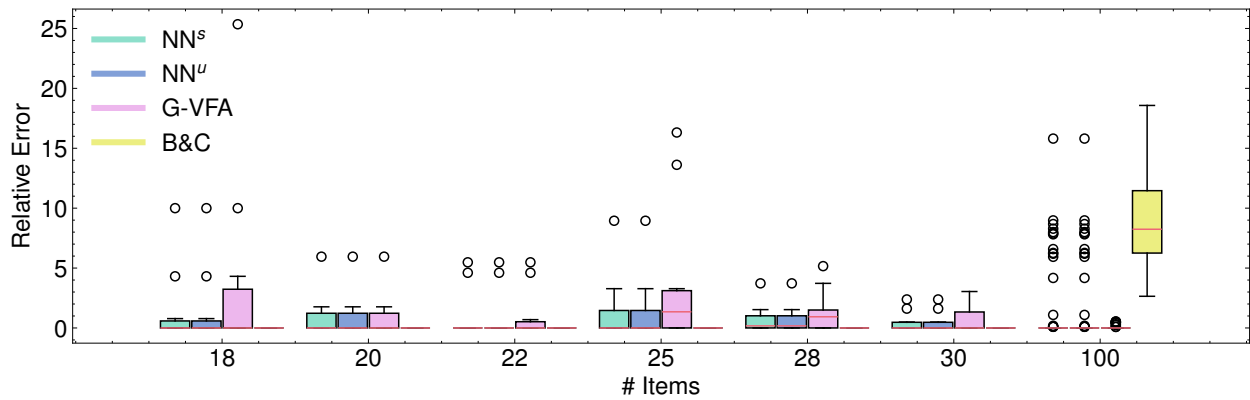


Figure 2: Box plot of relative errors for KIP with interdiction budget of $k = n/2$.

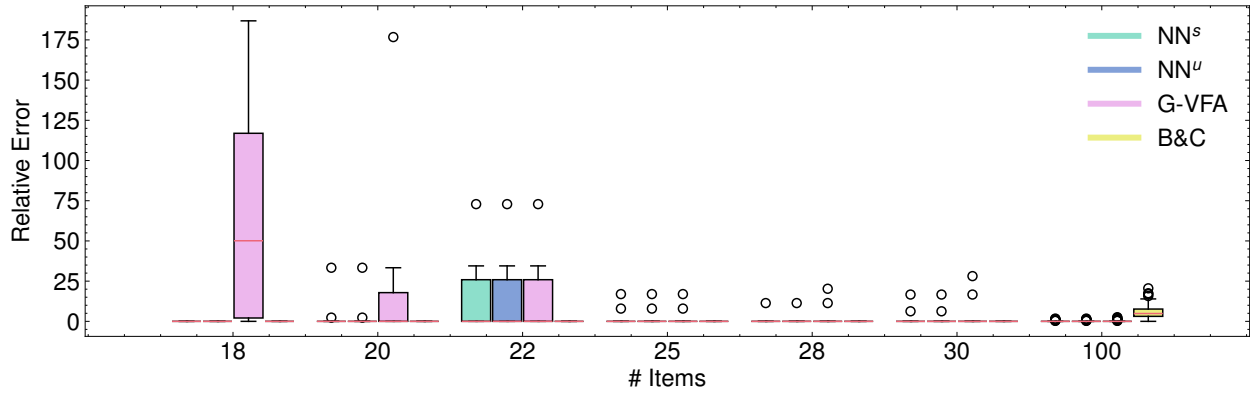


Figure 3: Box plot of relative errors for KIP with interdiction budget of $k = 3n/4$.

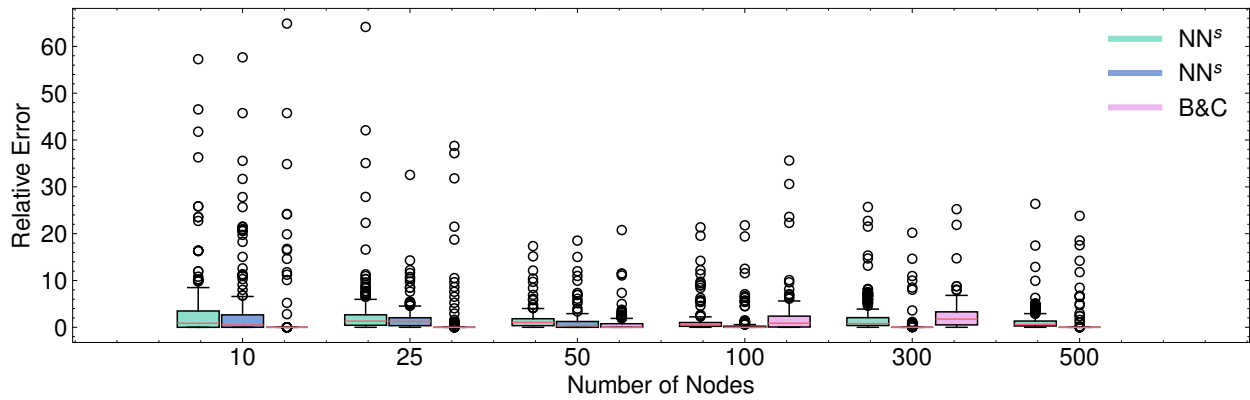


Figure 4: Box plot of relative errors for CNP.

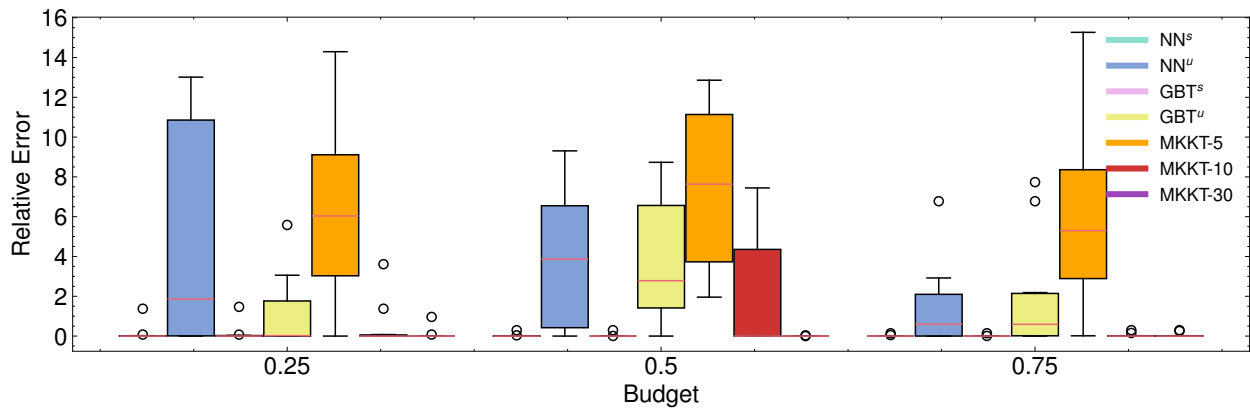


Figure 5: Box plot of relative errors for DNDP with 10 edges. MKKT- $\{5,10,30\}$ corresponds to MKKT run with each respective time limit.

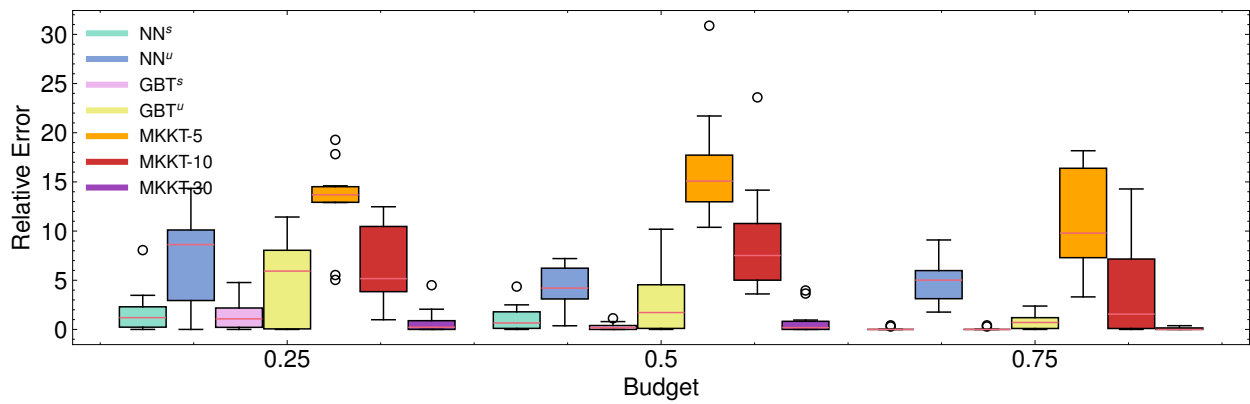


Figure 6: Box plot of relative errors for DNDP with 20 edges. MKKT- $\{5,10,30\}$ corresponds to MKKT run with each respective time limit.